

# QPS Confinement and Transport

Don Spong<sup>1</sup>, L. Berry<sup>1</sup>, S. Hirshman<sup>1</sup>, J. Lyon<sup>1</sup>,

D. Mikkelsen<sup>2</sup>,

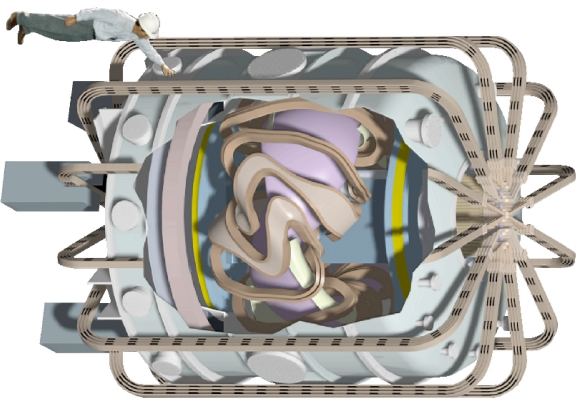
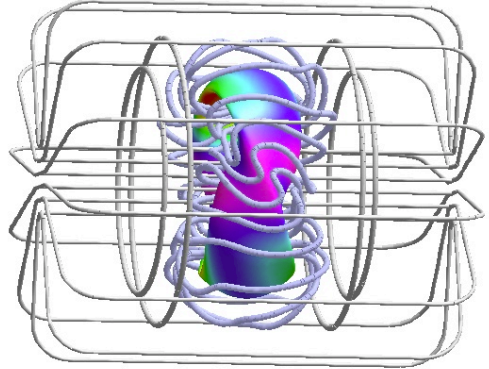
<sup>1</sup>Oak Ridge National Laboratory

<sup>2</sup>Princeton Plasma Physics Laboratory

## 13th INTERNATIONAL STELLARATOR WORKSHOP

Australian National University

Canberra, Australia



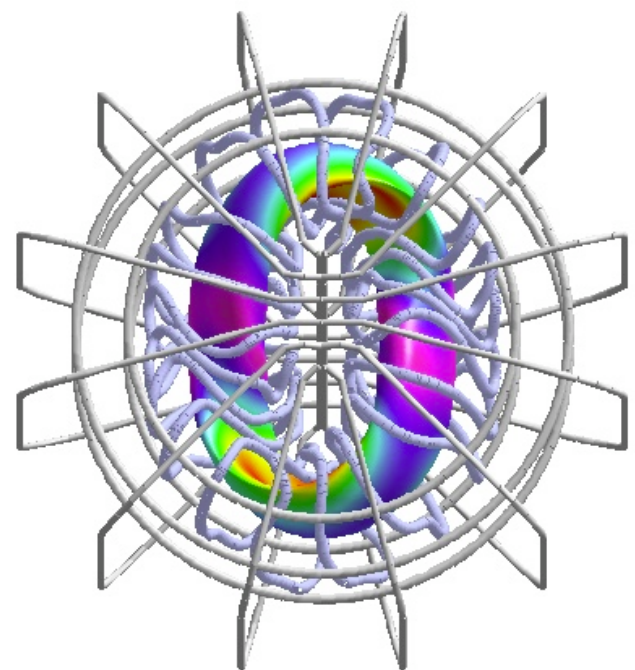
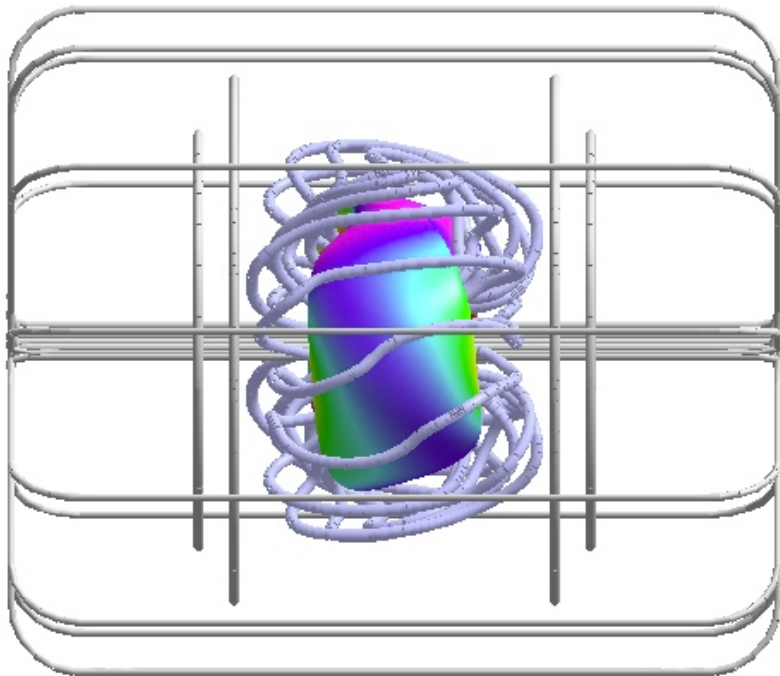
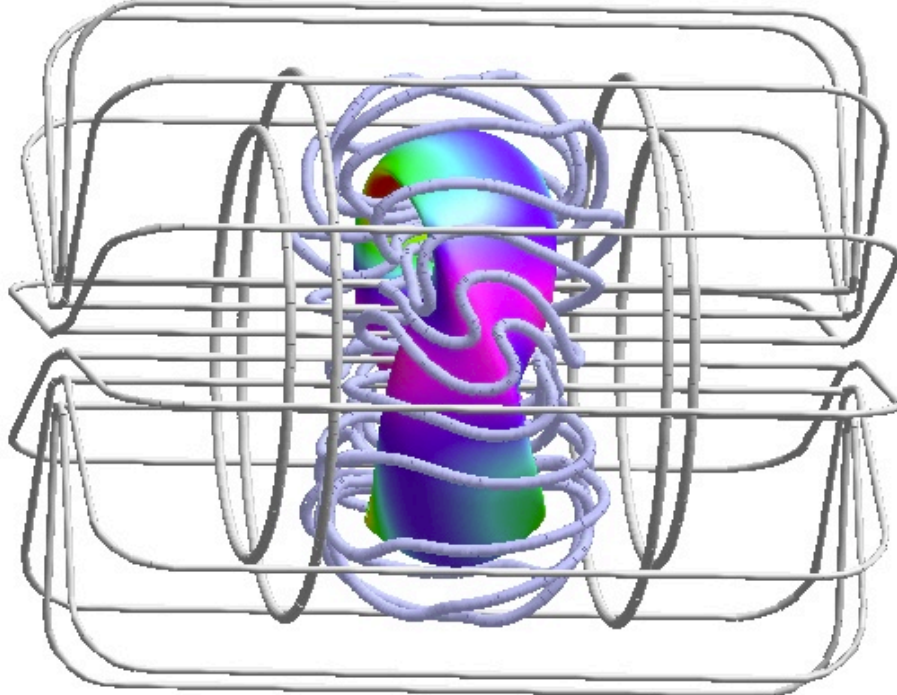
OAK RIDGE NATIONAL LABORATORY  
U.S. DEPARTMENT OF ENERGY



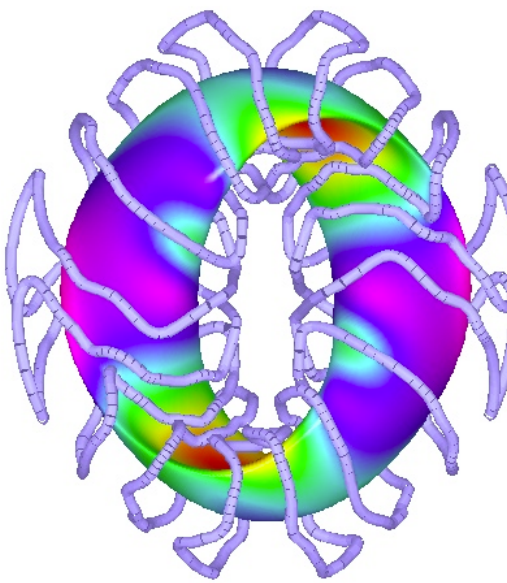
# QPS Confinement and Transport Topics

- Is neoclassical stellarator transport sufficiently subdominant to anomalous transport ( $\langle \Delta_{\text{heo}} \rangle >> \langle \Delta_{\text{ss95}} \rangle$ )?
  - to allow well defined enhanced confinement regimes
  - we consider both low (ECH) and high collisionality (ICRH) regimes
- Status of transport tools and QPS predictions
  - simple transport targets used in optimization
  - local diffusive transport models
    - DKES, NEO, 0-D, 1-D calculations
  - global Monte Carlo model
- Bootstrap current levels
  - To what extent do collisional/electric field effects modify bootstrap current?
  - Required incremental Ohmic currents
- Can significant  $\Delta$ 's be attained?
  - to test bootstrap current/equilibrium robustness
  - to test stability

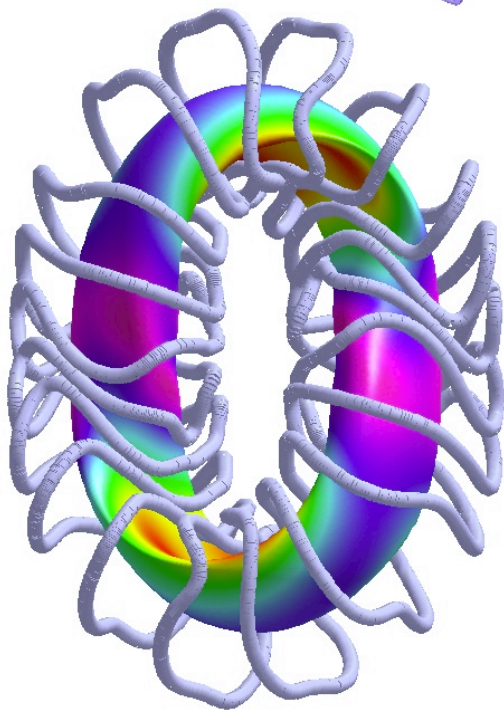
View of recent QPS configuration with modular, vertical and toroidal field coils:



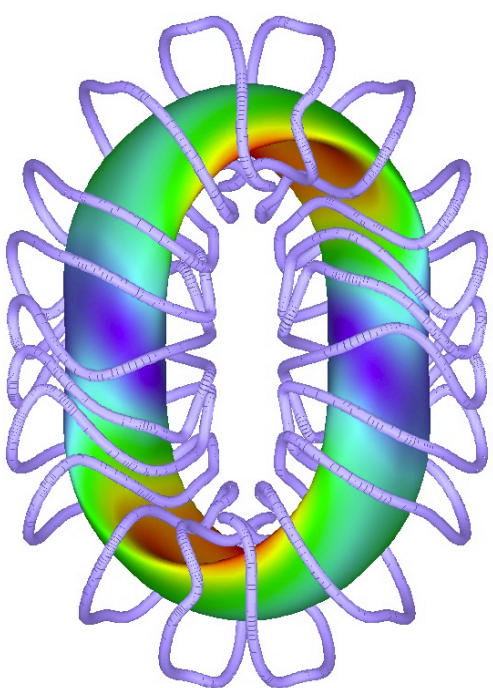
The QPS design has been evolving : several earlier QPS configurations are analyzed here



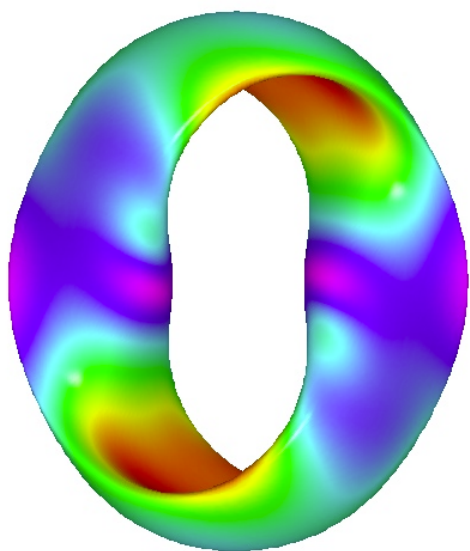
GB4 - PVR Ref.



Current  
1108a4



QPS 1016 4  
(similar to 926, 929)



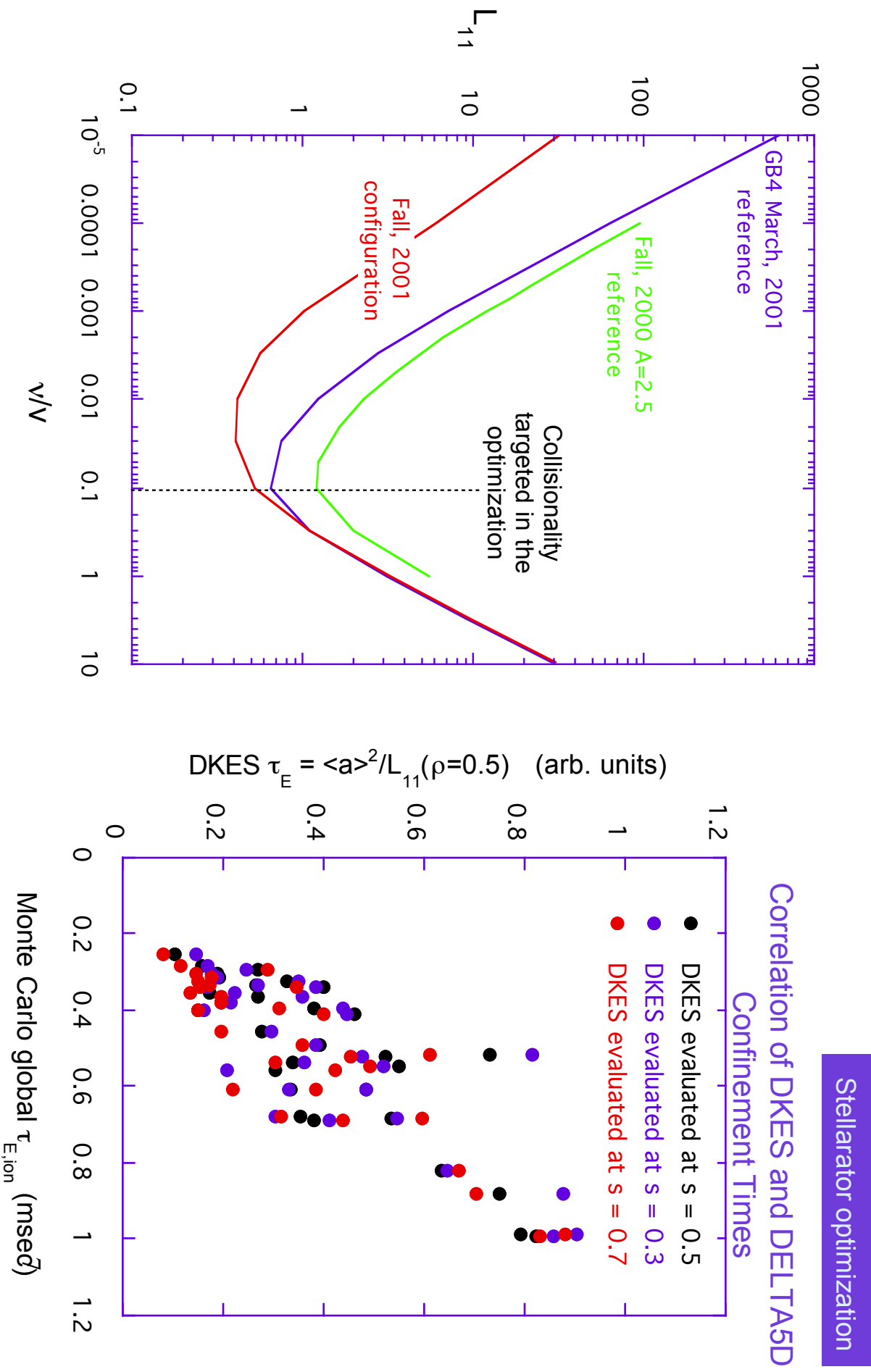
GB5

# *QPS TRANSPORT OPTIMIZATION*

# Transport Tools used to Evaluate QPS configurations:

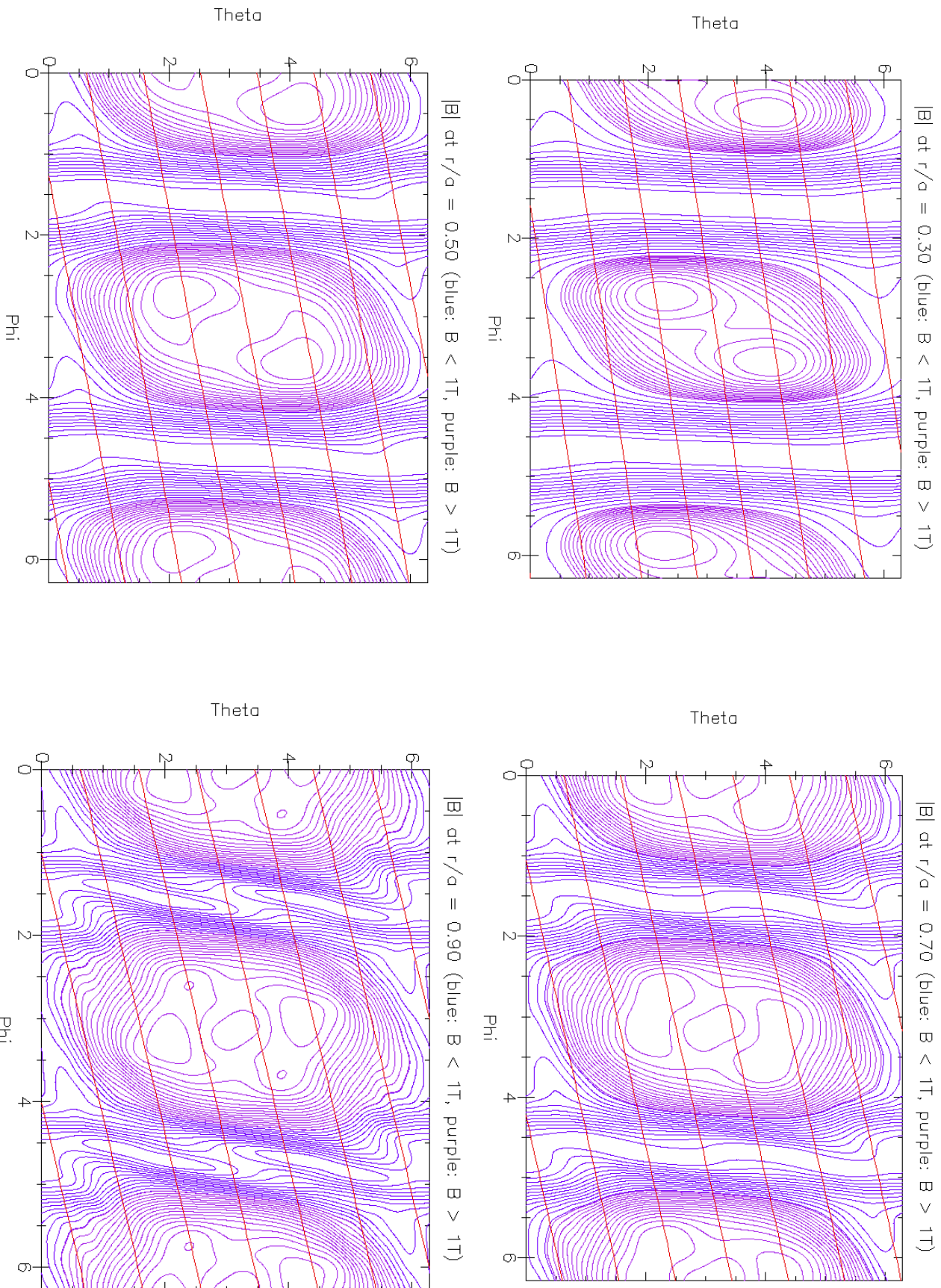
<b>Transport tool</b>	<b>Physical Model</b>	<b>Fixed Parameters</b>	<b>Predicted Parameters</b>
<b>0-D model</b>	ISS95	$P_{\text{heat}}, n$	$\Delta, \Delta_E, T$
<b>1-D model</b>	ISS95 + Simplified neoclassical	$P_{\text{heat}}(r), n(r)$	$T(r), \Delta, P_{\text{loss}}(r)$
<b>NEO</b>	$1/\Delta, E_r = 0$ neoclassical	$n', T'$	$\Delta_{\text{eff}}^{3/2}$
<b>DKES</b>	Local neoclassical	$n', T', E_r, \Delta$	Transport coefficient matrix
<b>Monte Carlo</b>	Large orbit global neoclassical	$N(r), T(r), \Delta(r)$	$\Delta_E, \Delta_b, \Delta_0$

# Transport optimizations using the NEO/DKES transport targets have resulted in confinement improvement.

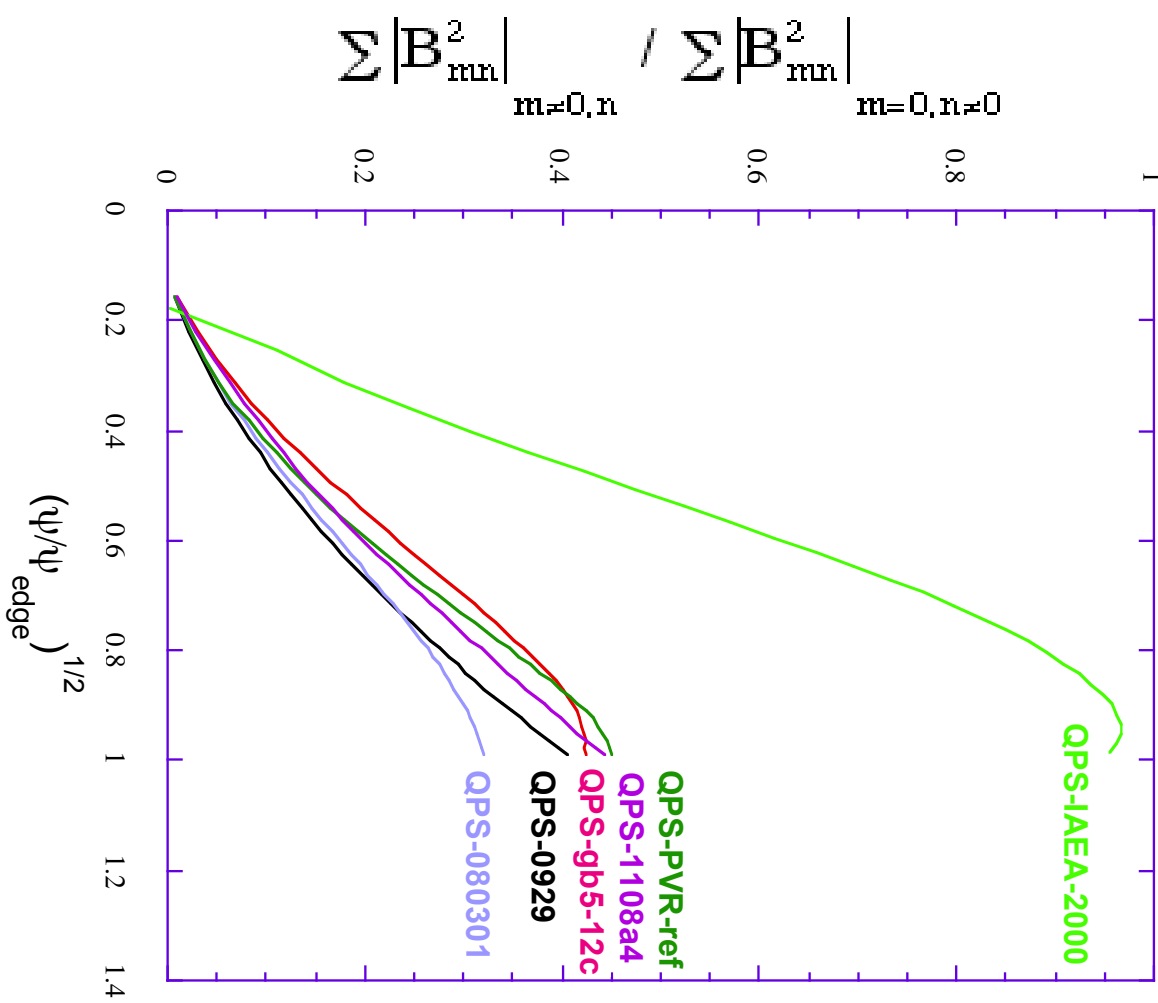


# *QPS MAGNETIC STRUCTURE*

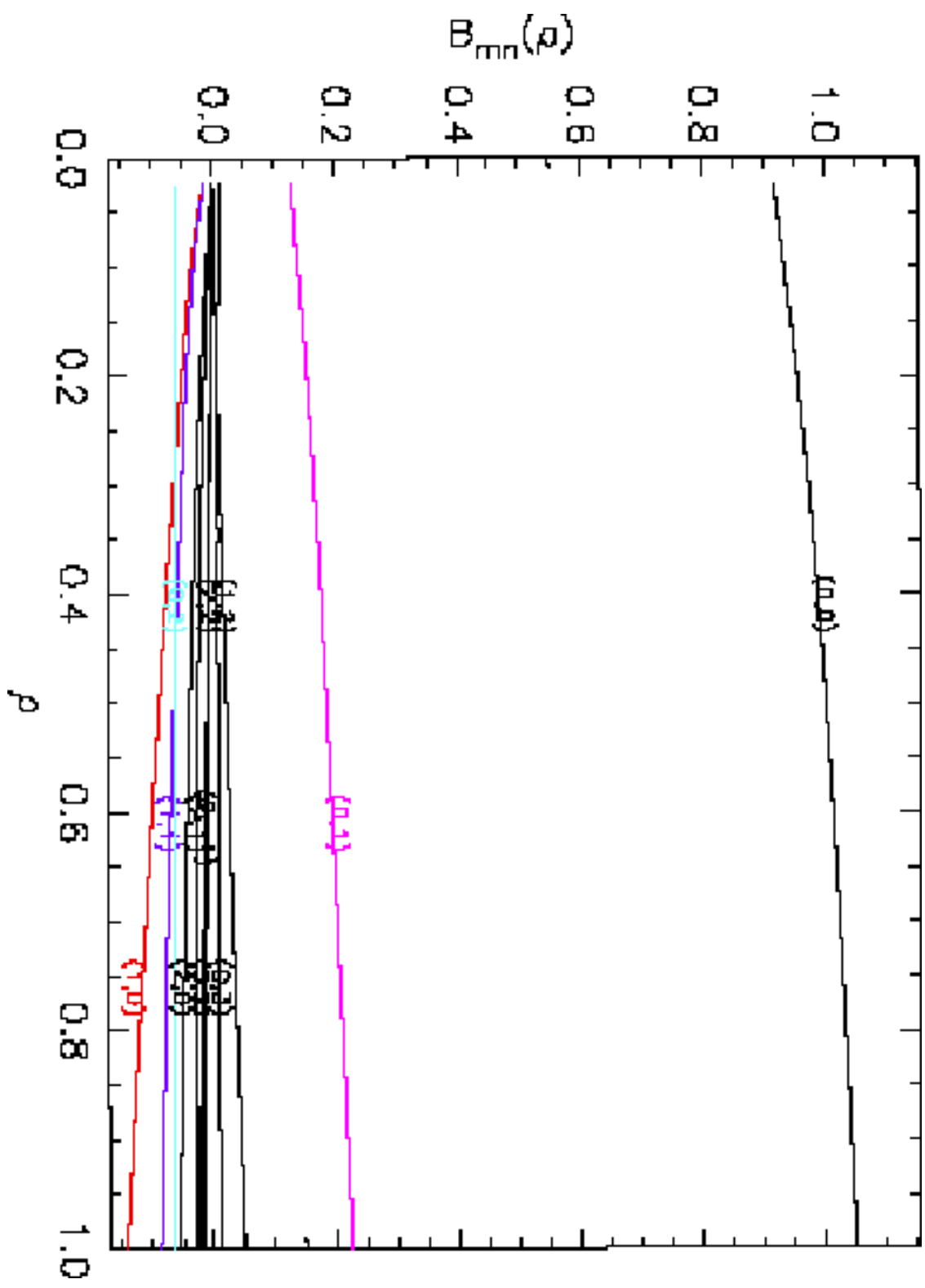
The variation of  $|B|$  on flux surfaces at “ $r/a$ ” = 0.3, 0.5, 0.7, 0.9 shows the quasi-poloidal symmetry about which QPS devices have been optimized:



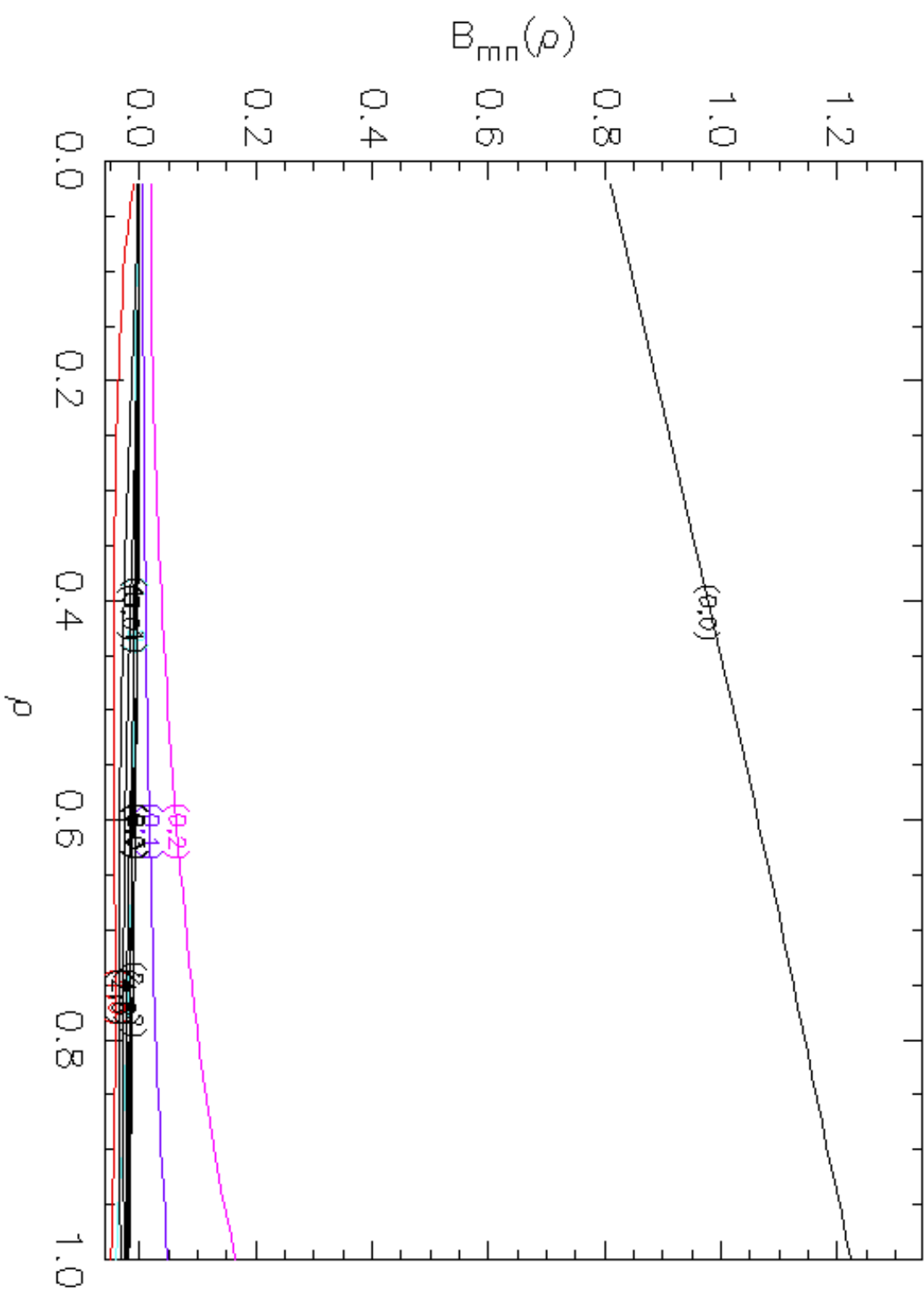
The ratio of magnetic energy in non-poloidally symmetric modes to the magnetic energy in poloidally symmetric modes (excluding  $m = n = 0$ ) is used as a measure of quasi-poloidal symmetry.



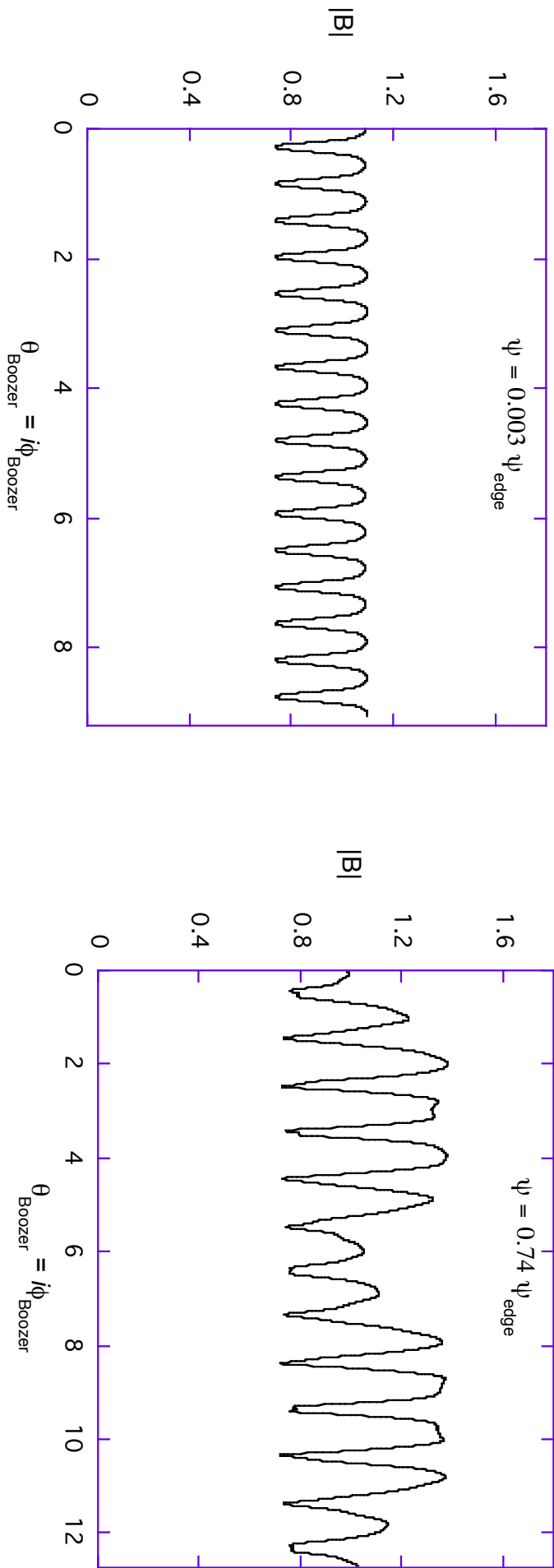
The  $B_{mn}$  spectrum for the QPS 1108a4 device shows that the dominant symmetry is in the poloidal direction



At high  $\Box$ 's ( $\equiv 15\%$  here) the QPS  $B_{mn}$  spectrum becomes increasingly quasi-poloidal.



Variation of  $|B|$  along a field line for QPS\_1016 configuration (near axis and edge): Minima are well aligned leading to good trapped particle confinement



# ***QPS O-D AND I-D TRANSPORT ANALYSIS***

# Global stellarator confinement scalings

$$\boxed{E}_{\text{ISS95}} = 0.079 H_{\text{ISS95}} a_p^{2.21} R^{0.65} P^{-0.59} n^{0.51} B^{0.83} \boxed{\mu}^{0.4}$$

$$\boxed{E}_{\text{ISS95}} = W_{\text{tot}} / P \quad W_{\text{tot}} = 1.5 <\boxed{\mu}> (\boxed{\mu}_0^2 / 2 \boxed{\mu}_0) V_p$$

0-D model

$$n_{\text{Sudo}} = 0.25 [PB / Ra_p^2]^{1/2}$$

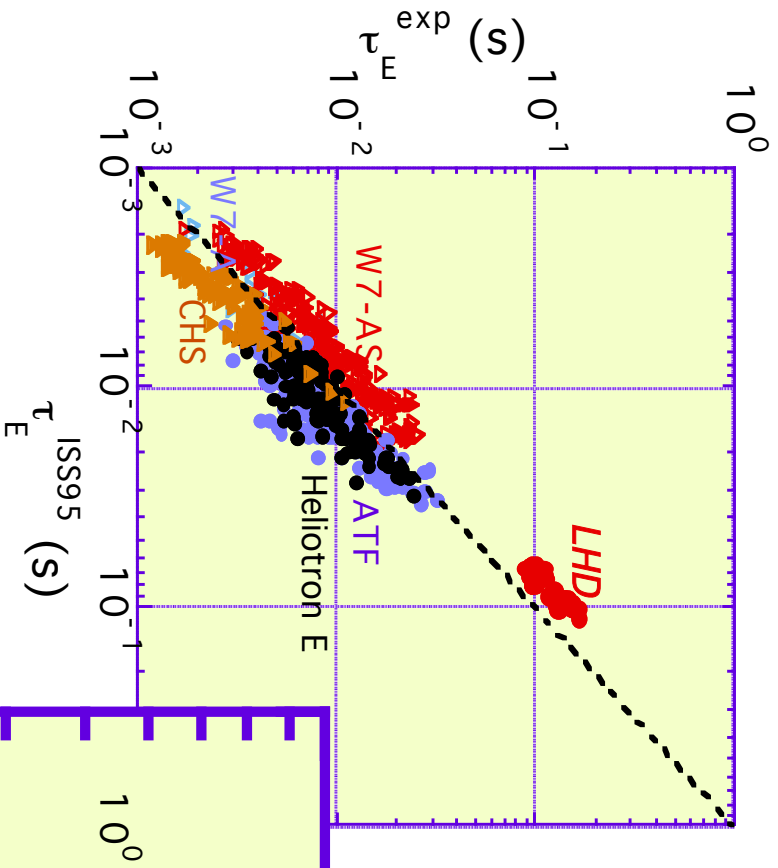
- Data only for  $R/a_p > 5$

- W7-AS and LHD find  
 $H_{\text{ISS95}}$  up to 2.5
  - low shear, large  $a_p$

- For fixed  $a_p, R, n, B, \boxed{\mu}$   
 can calculate:

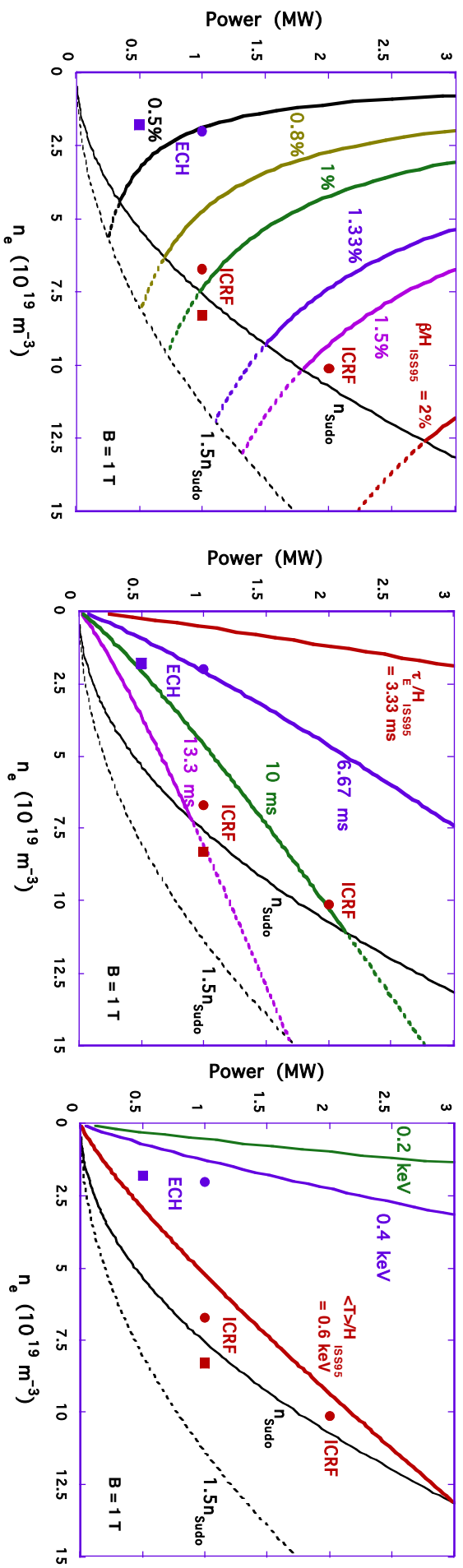
$$<\bar{T}>/H_{\text{ISS95}}$$

$$<\boxed{\mu}>/H_{\text{ISS95}}$$



# Global stellarator confinement scalings indicate the QPS CE device can achieve adequate plasma performance for its mission

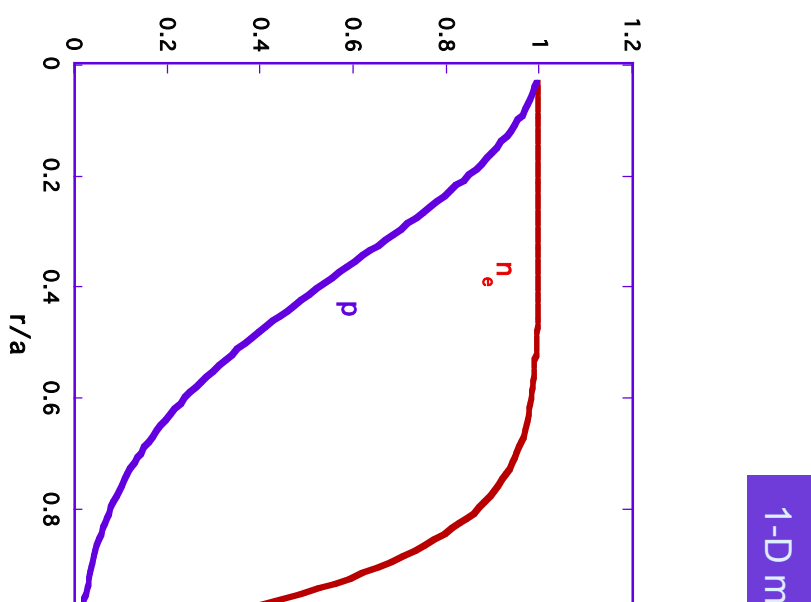
0-D model



# 1-D Model (Dave Mikkelsen) includes profile effects and self-consistent ambipolar electric field

- Coupled electrons/ion power balance equations
- Ambipolar particle balance for helical ripple component
- Thermal diffusivities
  - Neoclassical ripple coefficient using  $\bar{\Delta}_{\text{eff}}^{3/2}$  from NEO code
  - $E_r$  dependence from Shaing-Houlberg single helicity model
- Density and power deposition profiles assumed as shown

This model has been motivated by more comprehensive calculations (DKEs, Monte Carlo)

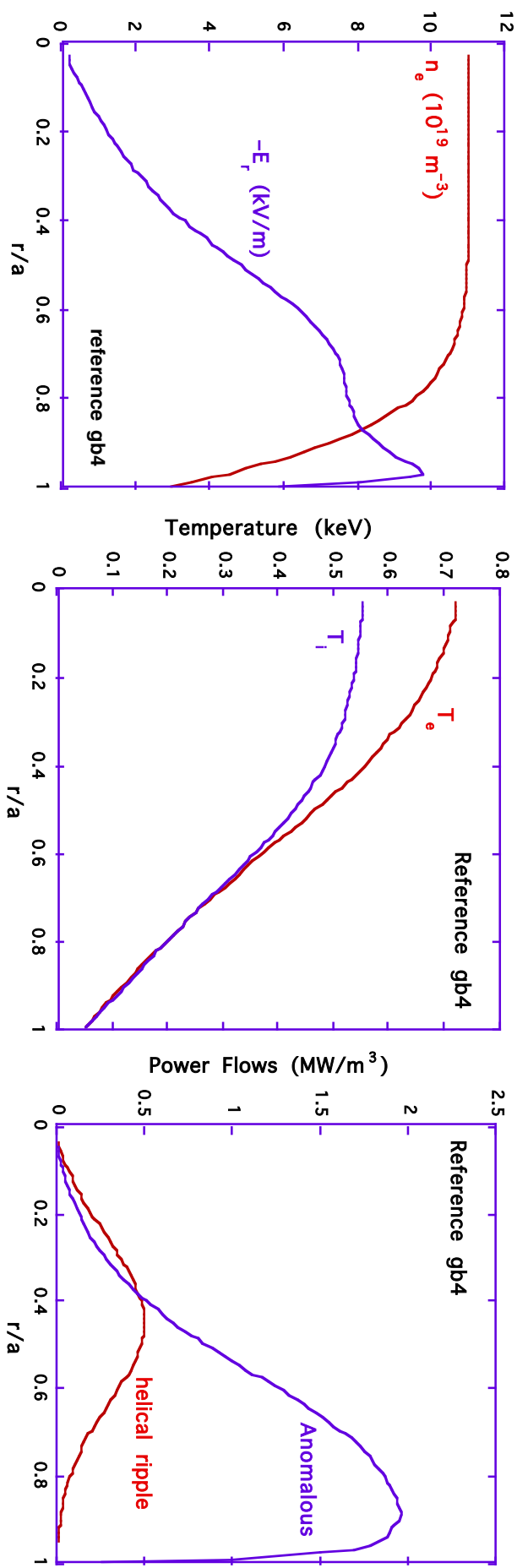


# ICRF Heated plasmas

**Device**       $\Delta E$  (msec)       $\langle \Delta E \rangle$       1-D model

gb4	18.3	1.4	
gb5_12c	18.8	1.44	
gb5_12d	18.9	1.46	

For  $B = 1\text{T}$ ,  $P_{\text{ICRF}} = 1\text{MW}$



# ECRF Heated plasmas - gb4 configuration

**Device**

$\Delta t(\text{msec})$

$\Delta t$

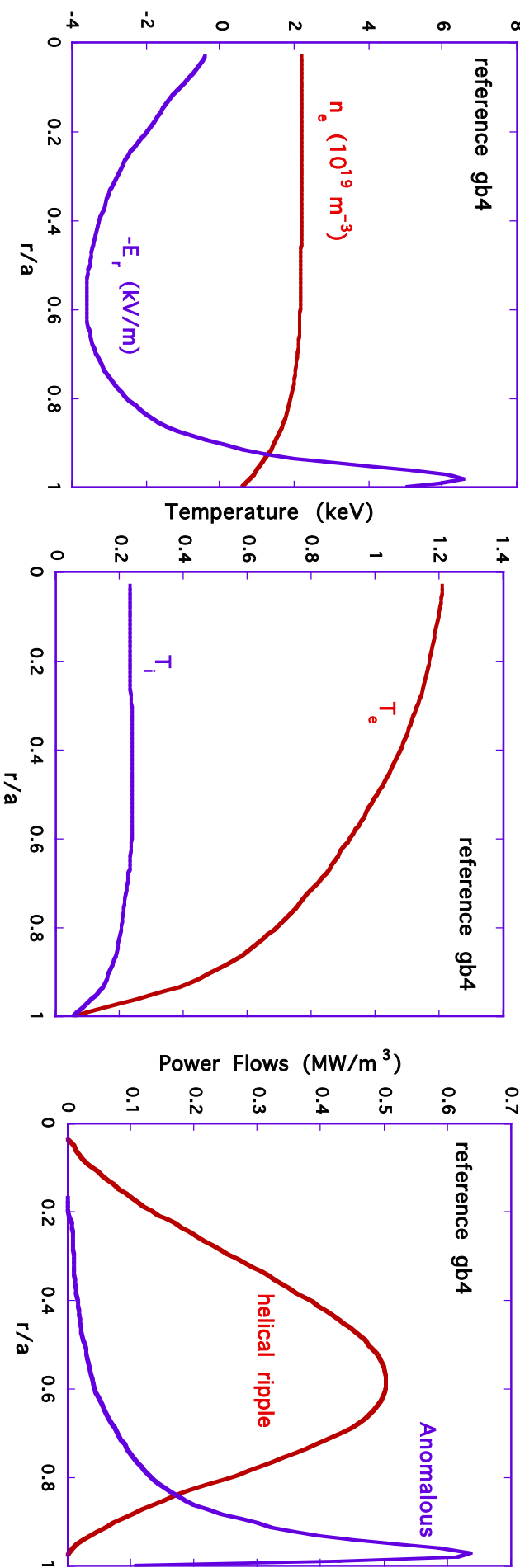
1-D model

gb4

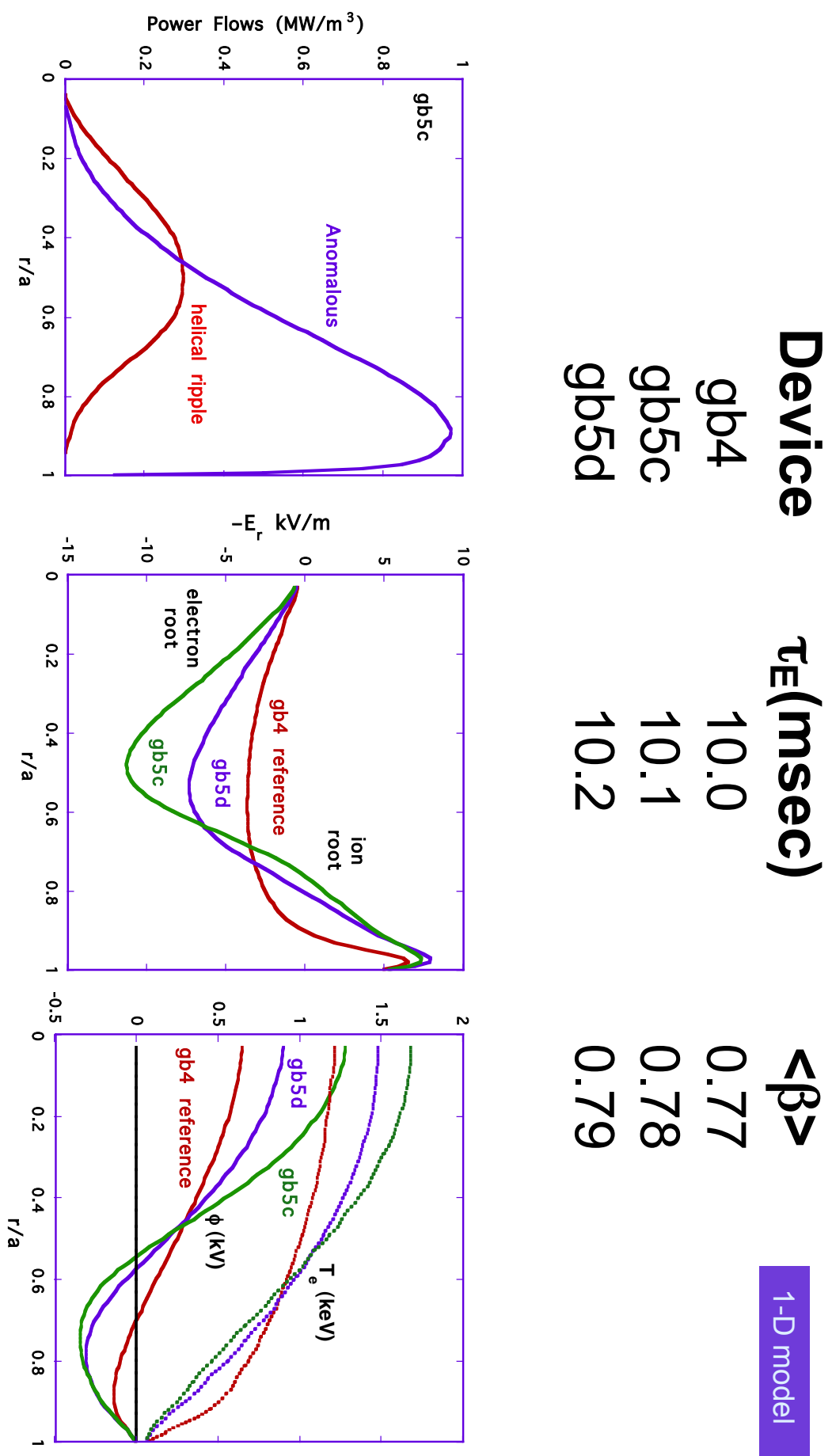
10.0

0.77

For  $B = 1\text{T}$ ,  $P_{\text{ECRF}} = 1\text{MW}$



**ECRF Heated gb5 configuration has helical ripple component that is subdominant to anomalous**



# *QPS DKES AND NEO TRANSPORT ANALYSIS*

# The DKES (Drift Kinetic Equation Solver) provides the full neoclassical transport coefficient matrix (multi-helicity)

DKES Transport analysis

$$\begin{aligned}
 \vec{D} &= \frac{3}{2} \frac{T}{T} \frac{eE_r}{T} \\
 I_i &= \frac{1}{T} \vec{Q} \cdot \vec{D}_s \\
 I_i &= \sum_{j=1}^3 \hat{D}_{ij} A_j \\
 \langle (\bar{u} \cdot \bar{u}_s) \cdot \vec{B} \rangle &= \frac{T}{T} \frac{\langle E \cdot \vec{B} \rangle}{\langle B^2 \rangle}
 \end{aligned}$$

$$\hat{D}_{ij} = n \frac{2}{\sqrt{I}} \int_0^\infty dK \sqrt{K} e^{\pm K} g_i g_j D_{ij}$$

where  $g_1 = g_3 = 1$ ,  $g_2 = K$ ,  $K = \frac{v}{V_{th}}^2$

- W. I. Van Rij, S. P. Hirshman, Phys. Fluids B 1, 563 (1989)

- Variational: provides upper and lower bounds on  $dS/dt$

$$D_{11} = D_{12} = D_{21} = D_{22} = \frac{V_{th}}{2} \frac{B_{V_{th}}}{B} \frac{d}{dr} \left[ \frac{B}{K} \right] K \sqrt{K} L_{11}$$

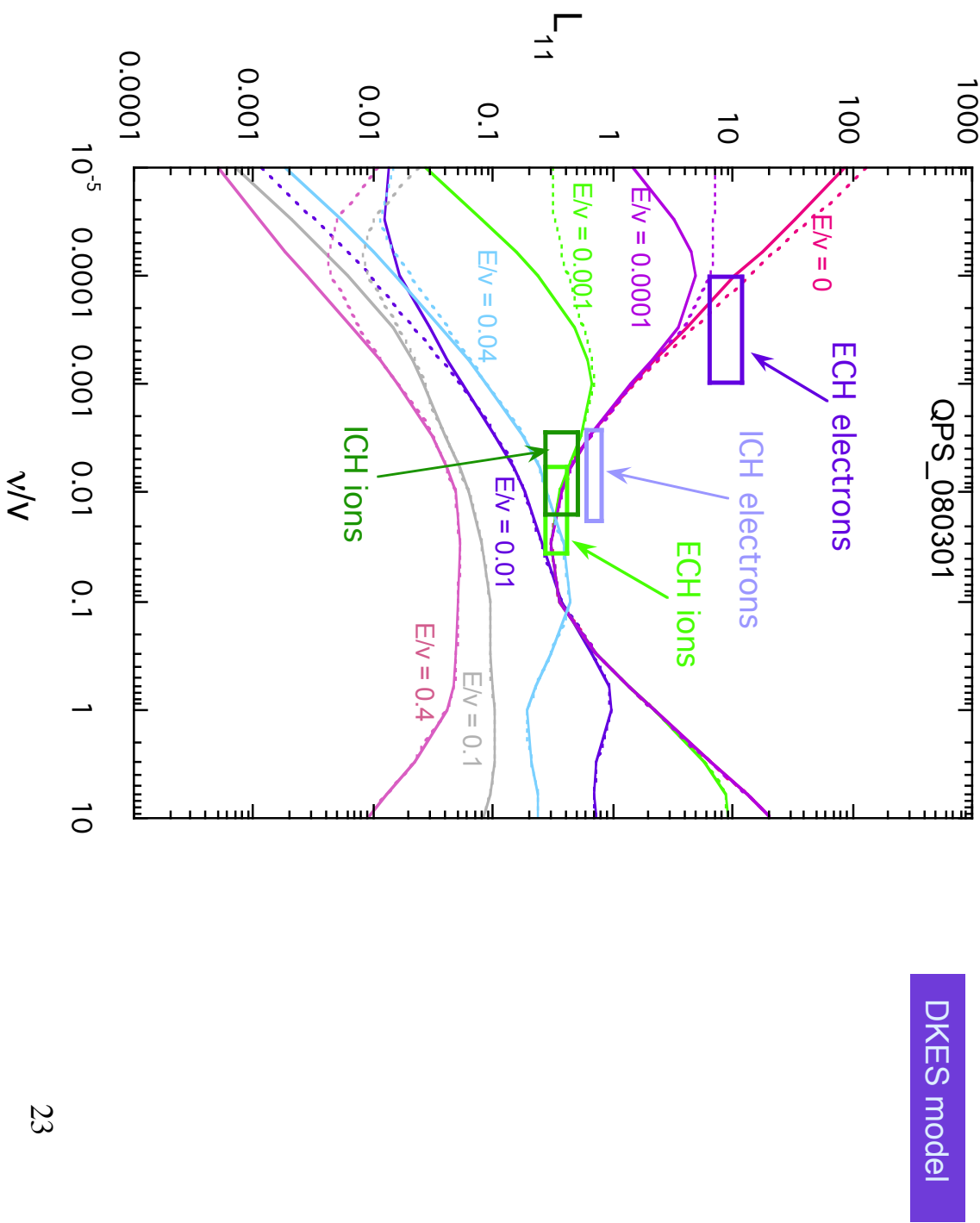
- Expands f in Fourier-Legendre series

$$D_{31} = D_{32} = \frac{1}{2} D_{13} = \frac{1}{2} D_{23} = \frac{V_{th}}{2} \frac{B_{V_{th}}}{B} \frac{d}{dr} \left[ \frac{B}{K} \right] K L_{31}$$

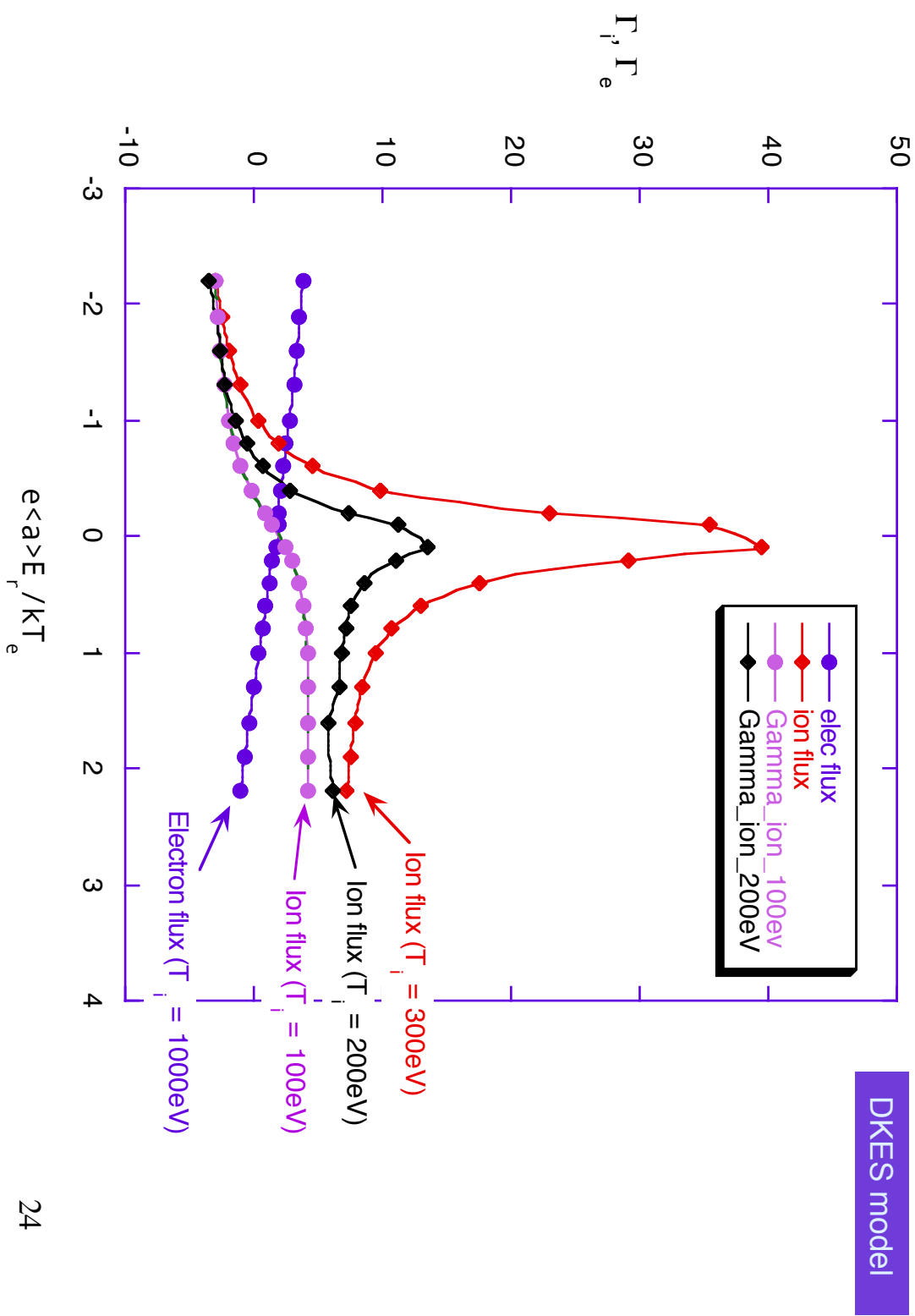
$$D_{33} = \frac{V_{th}}{2} \sqrt{K} L_{33}$$

(i.e., to carry out the above integrals, one will need to generate a 2-D matrix of  $\square$ 's vs. these parameters for each flux surface)

This model is motivated by the more complete DKES calculations that indicate electrons are generally in the  $1/\Box$  regime:

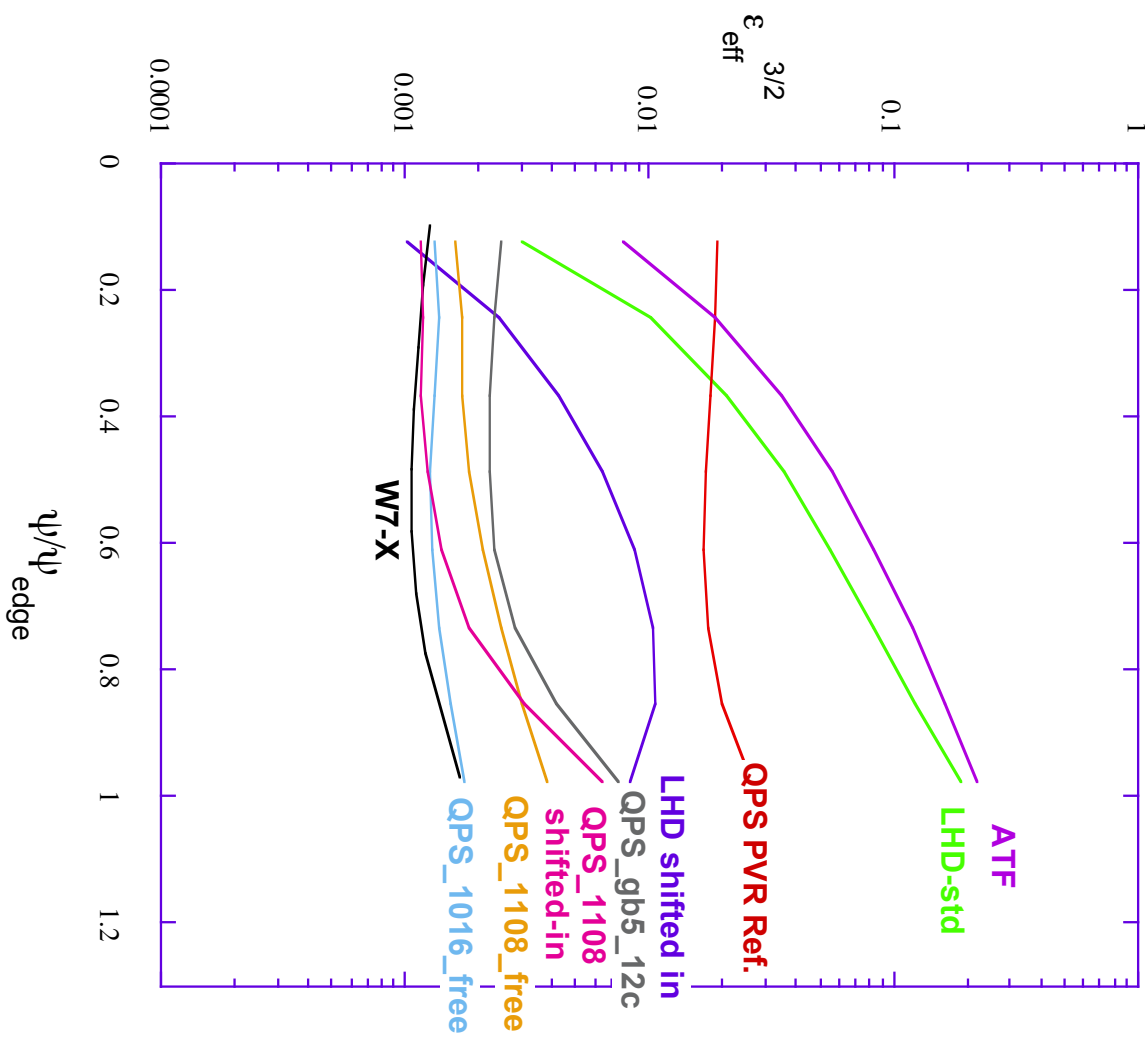


Typical DKES ambipolar calculations also show that overall transport level is generally set by lowering ion flux down to that of the electrons.

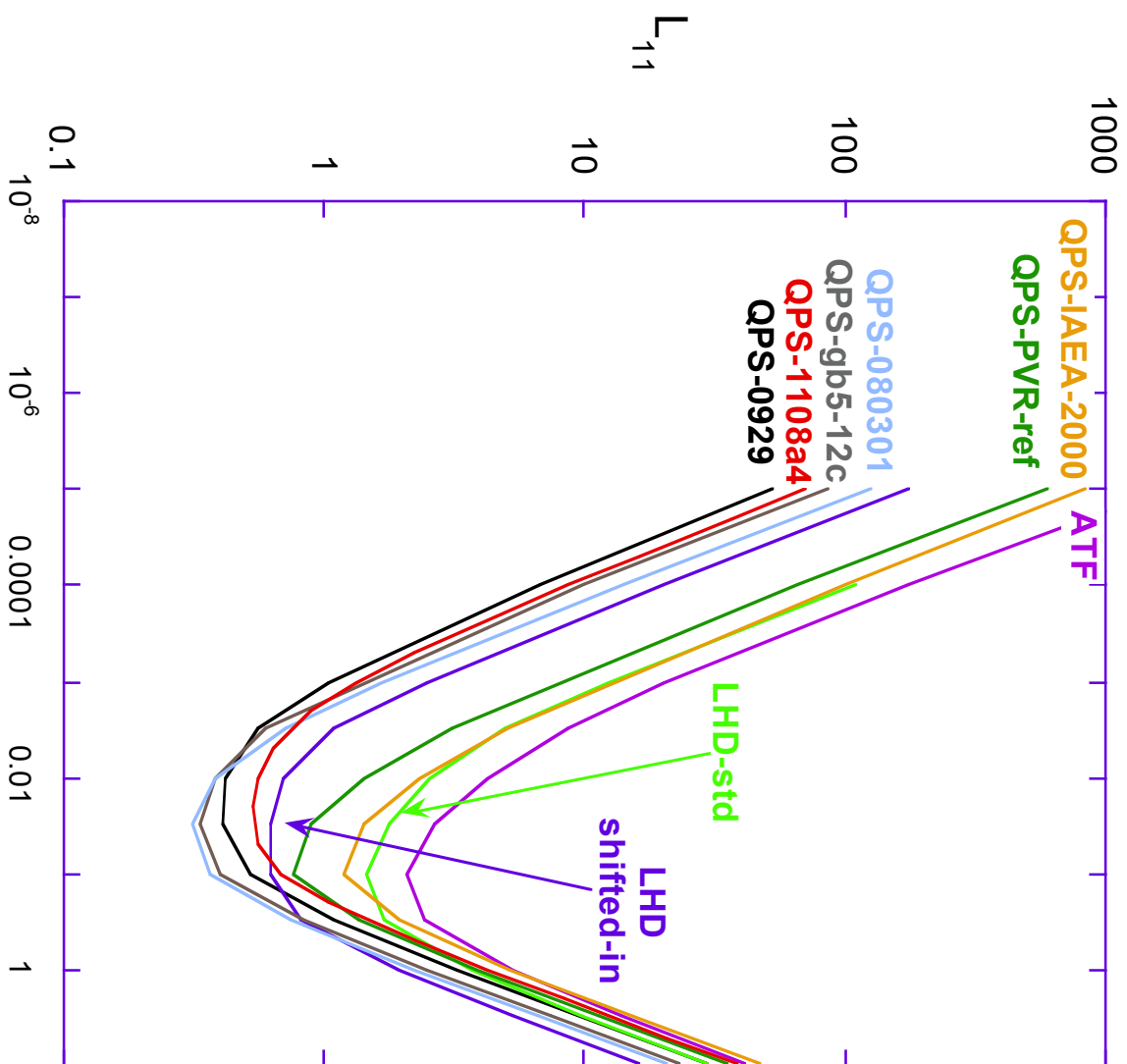


**NEO code provides  $\square_{\text{eff}}^{3/2} \sim D^{1/\square}$ ,  $\square^{1/\square}$ . Demonstrates effectiveness of NEO/DKES optimizations over a series of configurations**

**NEO  $\square_{\text{eff}}$  code**



DKES  $L_{11}$  transport coefficient at  $E_r/V = 0.0001$  show similar trends at low collisionality among gb4/gb5 devices as NEO  $\Delta_{\text{eff}}^{3/2}$  coefficient

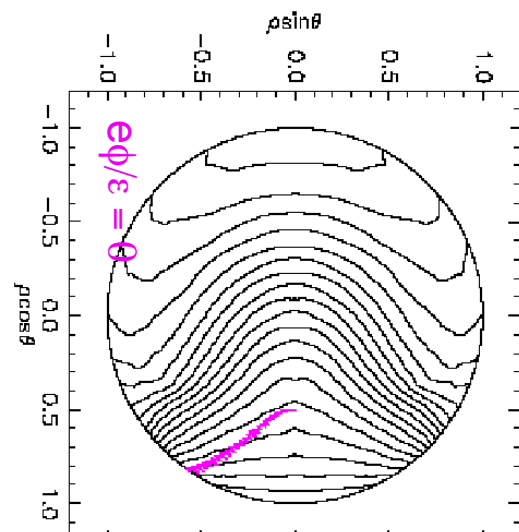
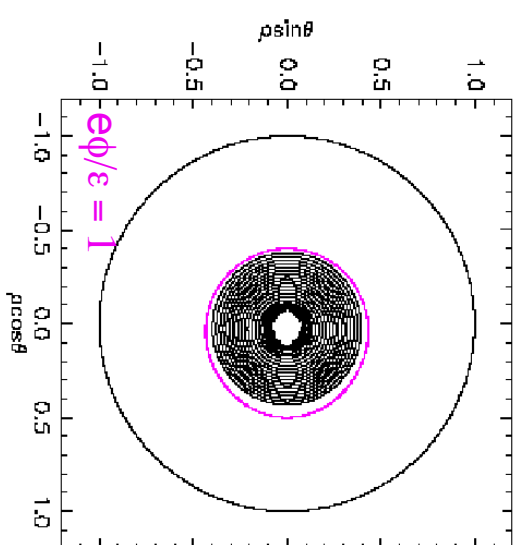
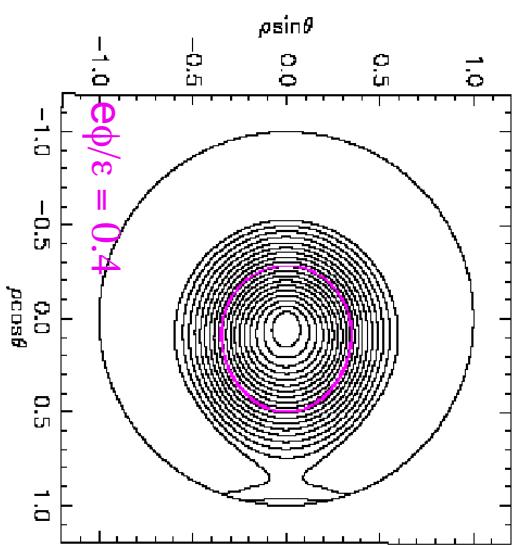
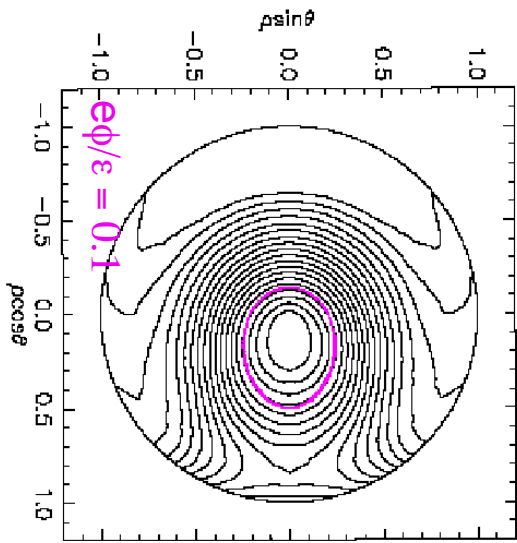
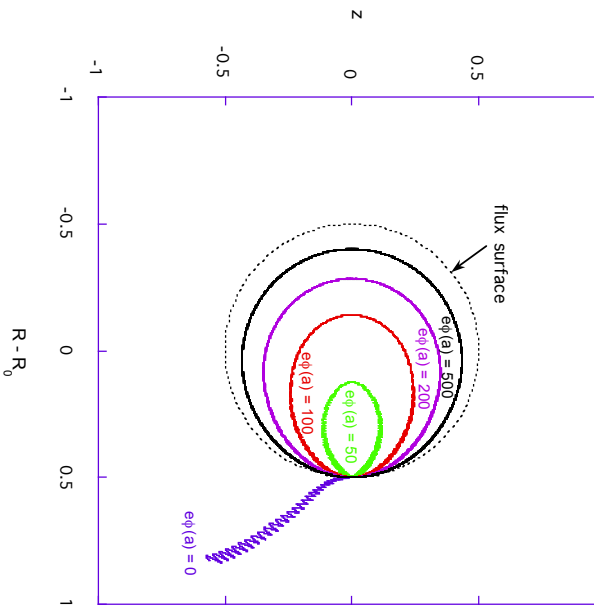


# *QPS ORBITS AND MONTE CARLO SIMULATION*

## Orbit trajectories

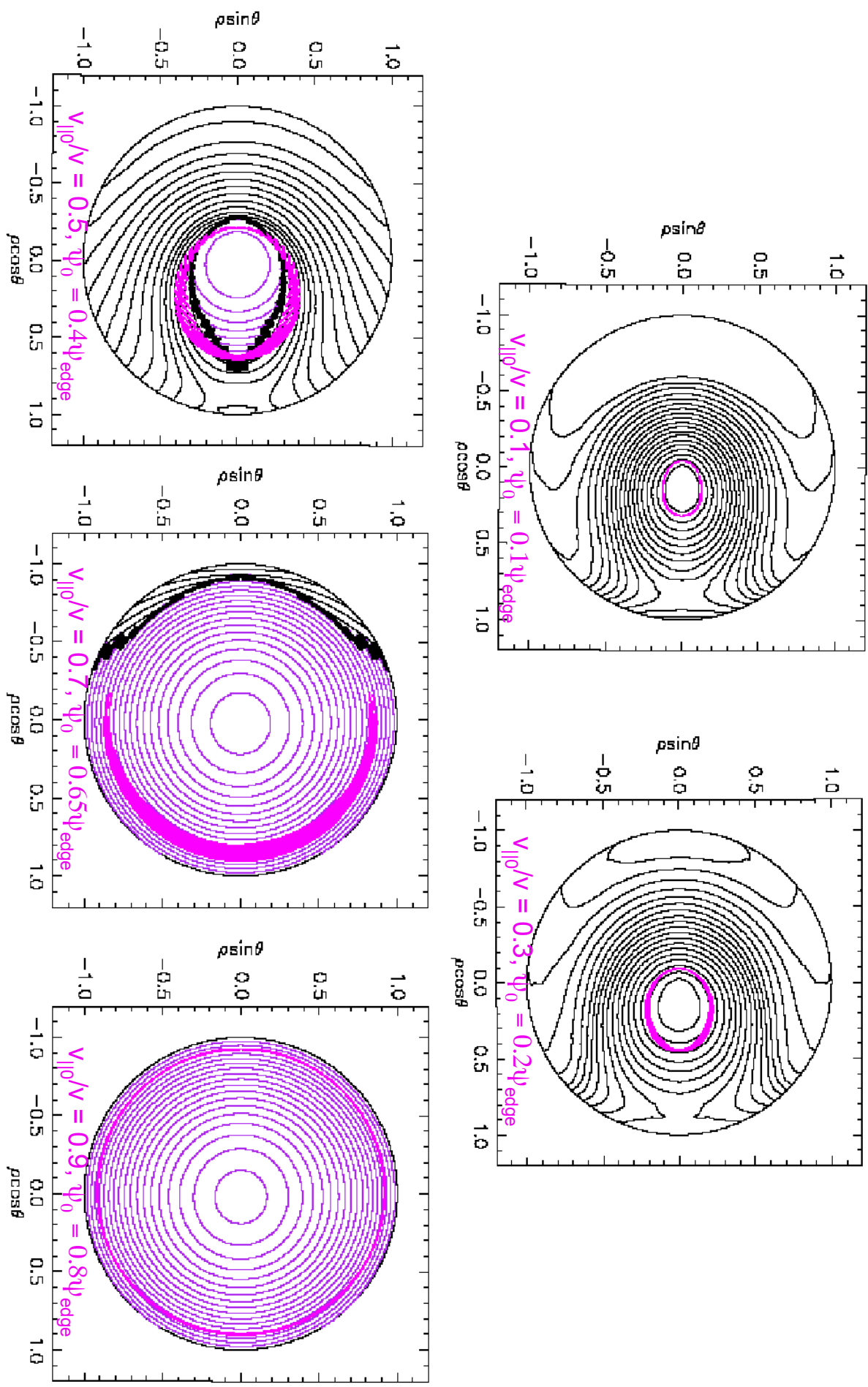
# Improvement of trapped 500 eV ion orbits with electric fields and alignment with $J^*$ contours

500 eV ion orbit in gb4\_nesc\_12b  
(initial conditions:  $r_{\text{ia}} = 0.5$ ,  $v_{\parallel}/v = 0.1$ )



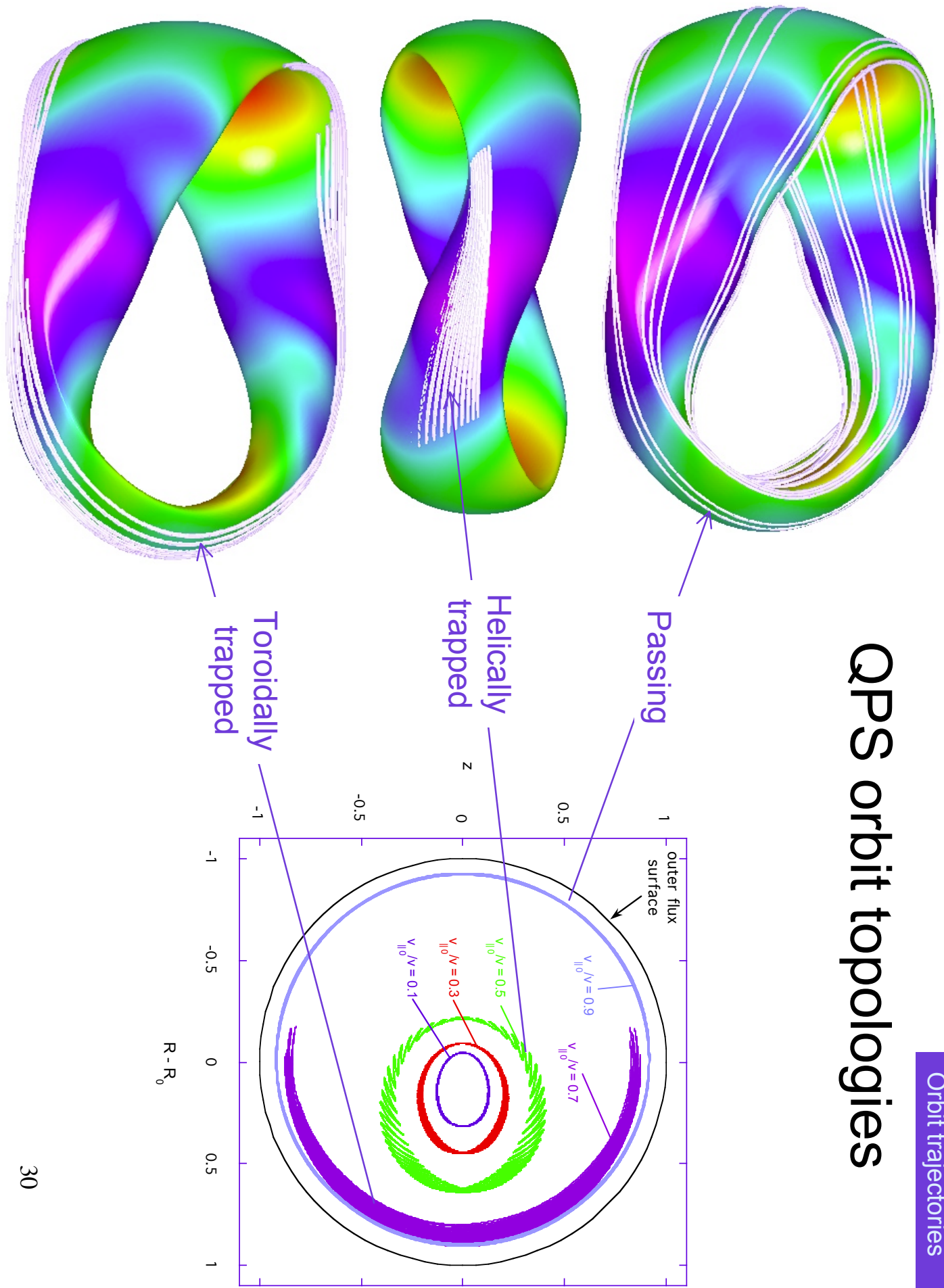
# Alignment of $v_{||0}/v = 0.1, 0.3, 0.5, 0.7, 0.9$ 500 eV ion orbits with $J^*$ contours

(black contours = locally trapped, purple contours = passing, magenta = orbit)



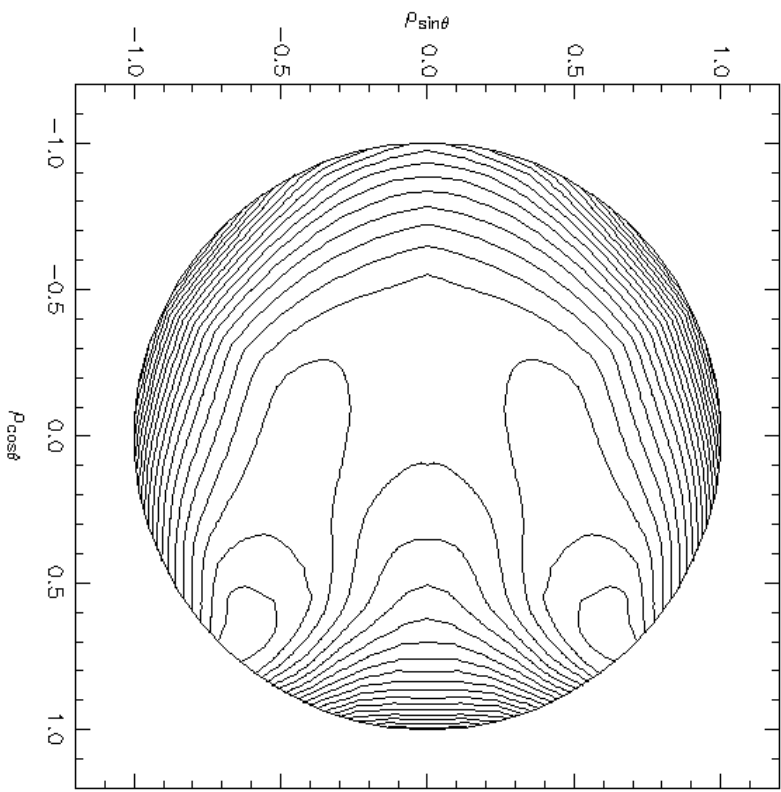
# QPS orbit topologies

Orbit trajectories

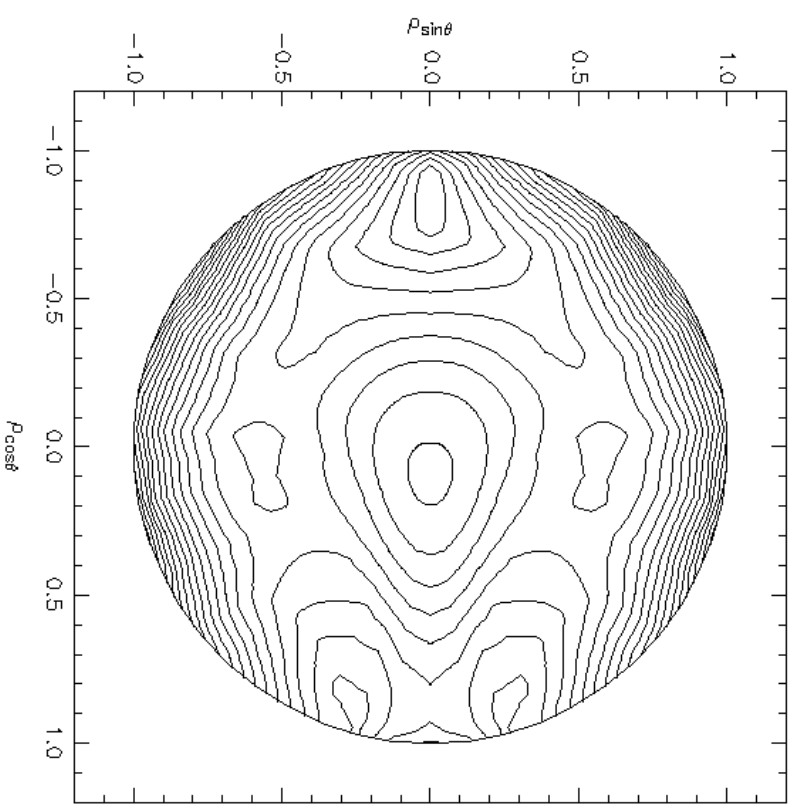


The recent QPS-1016 configuration improves the closure and centering of  $B_{\min}$  contours:

QPS-GB5



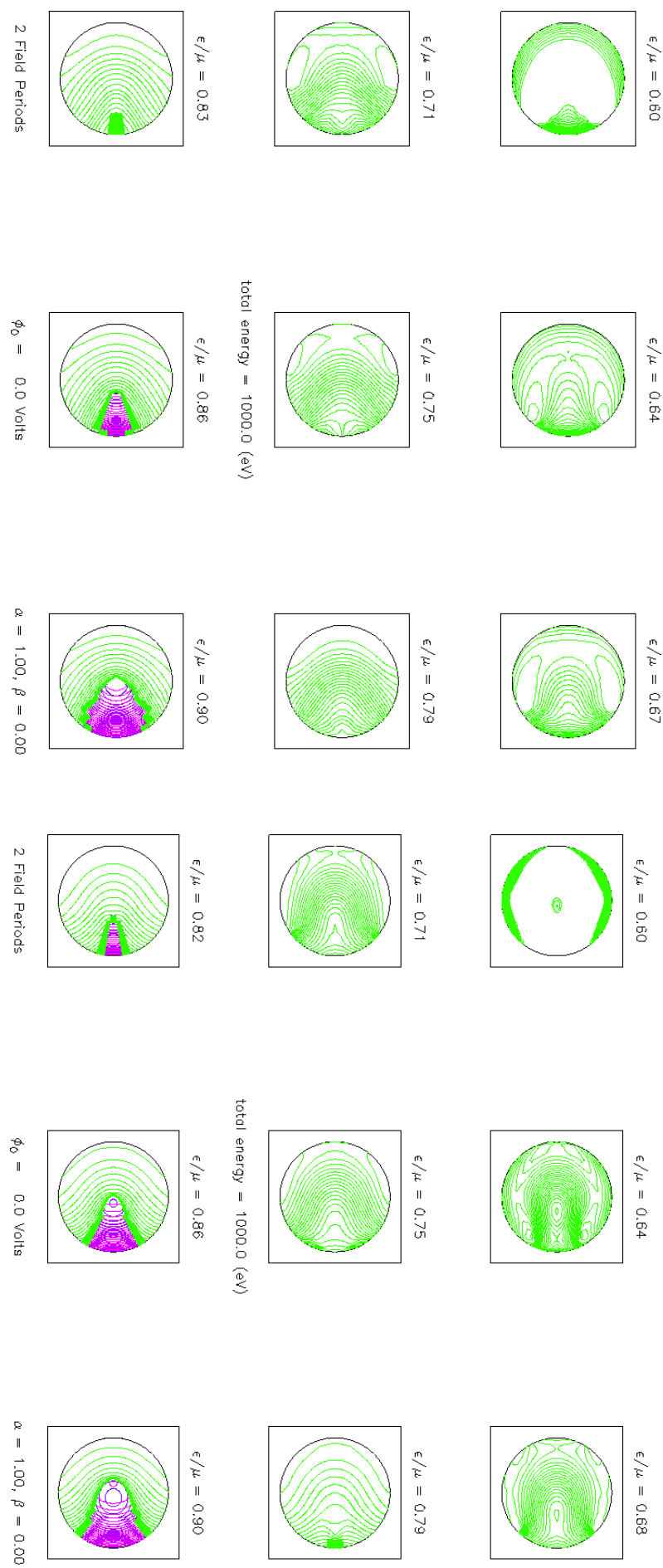
QPS-1016



QPS-1016 also improves closure of the deeply traped  $J^*$  contours ( $|J| < 0.7$ )

QPS-GB5

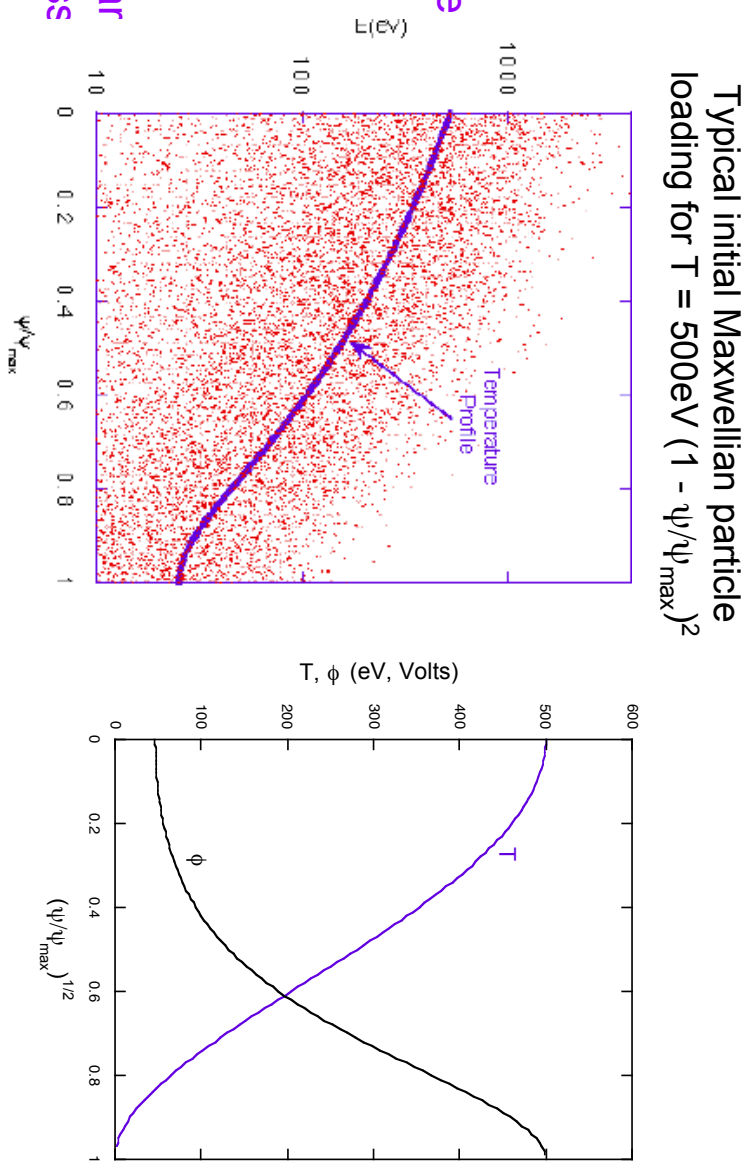
QPS-1016



# Monte Carlo procedure for estimating global energy lifetimes (DELTA5D code)

DELTA5D Monte Carlo

- start with particles distributed over cross section using PDF's consistent with assumed profiles and local Maxwellians
- follow ensemble in time, replacing particles (consistent with initial PDF's) as they leave outer surface
- Record energies of escaping particles - use to calculate  $\bar{E}$
- Follow until approximate steady-state is achieved
- Vary potential (with fixed profile shape) to achieve global ambipolar balance of electron/ion particle loss rates



## Power flows for global single species test particle simulations:

DELTA5D Monte Carlo

- To achieve steady state, in a reasonable simulation time, terms (1) and (2) need to be balanced:
- For  $E_r = 0$ 
  - can include pitch angle and energy scattering if  $Q_{ii} + Q_{ei}$  is weak during particle confinement time
  - or can include only pitch angle scattering
- For  $E_r \neq 0$ 
  - rely on  $Q_{ii} + Q_{ei}$  term (1) to redistribute energy loss/gain from term (2)
  - or can remove kinetic energy loss/gain (due to e $\square$ ) each time step

$$\frac{dW_{test,ion}}{dt} = \int (Q_{ii} + Q_{ei}) d^3v \quad (+/-) \quad (1)$$

$$+ \int \vec{J} \bullet \vec{E} d^3v \quad (+/-) \quad (2)$$

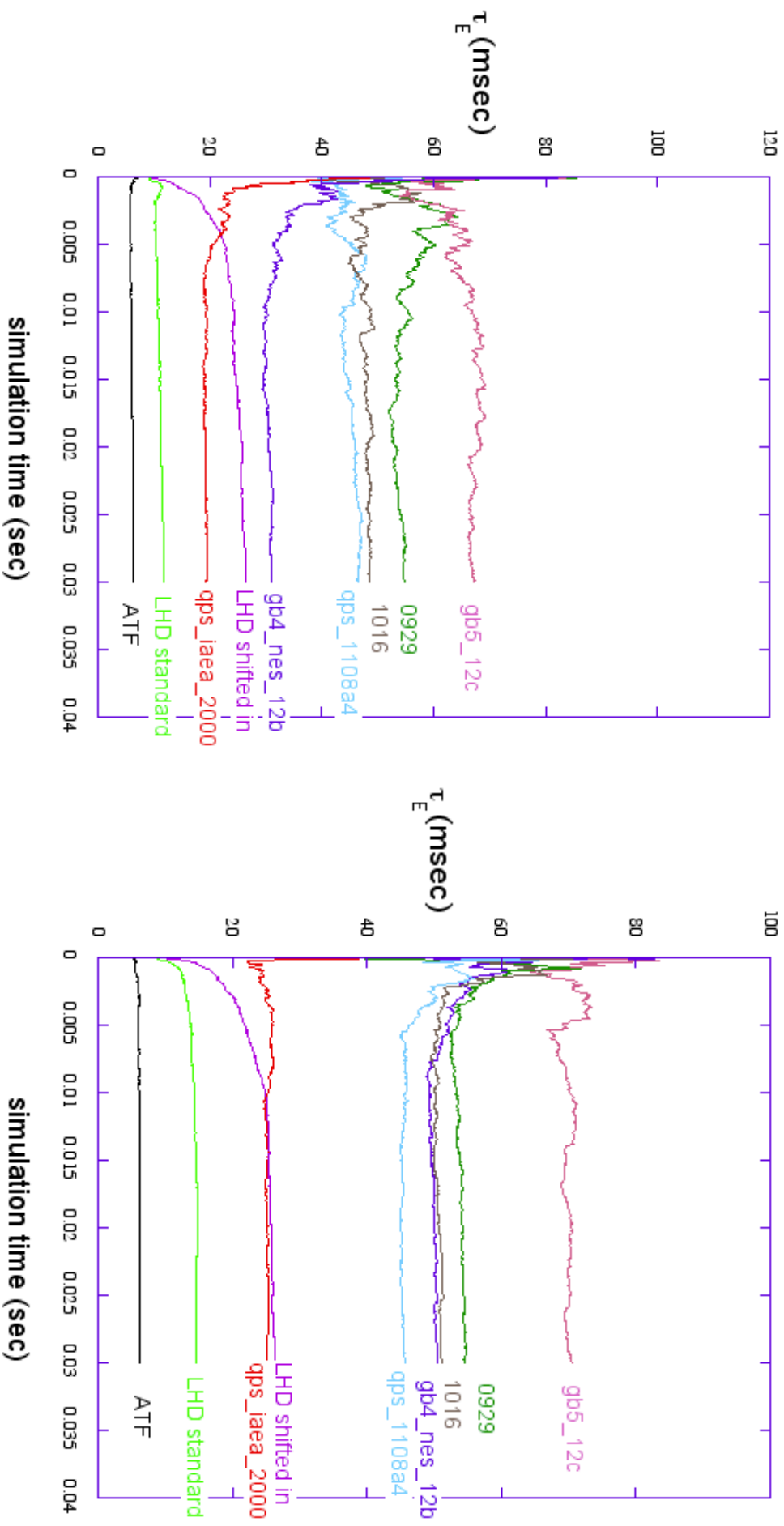
$$+ \int \frac{dW_{surface\ loss}}{dt} dS \quad (-) \quad (3)$$

$$+ \int N_{replacement} [T(\square) + e\square] d^3v \quad (+/-) \quad (4)$$

$$\frac{dW_{test, electron}}{dt} = \text{Similar equations}$$

# Comparison of Ion Monte Carlo lifetimes among different configurations (all scaled to constant $R_{\max}$ and $\langle B \rangle$ )

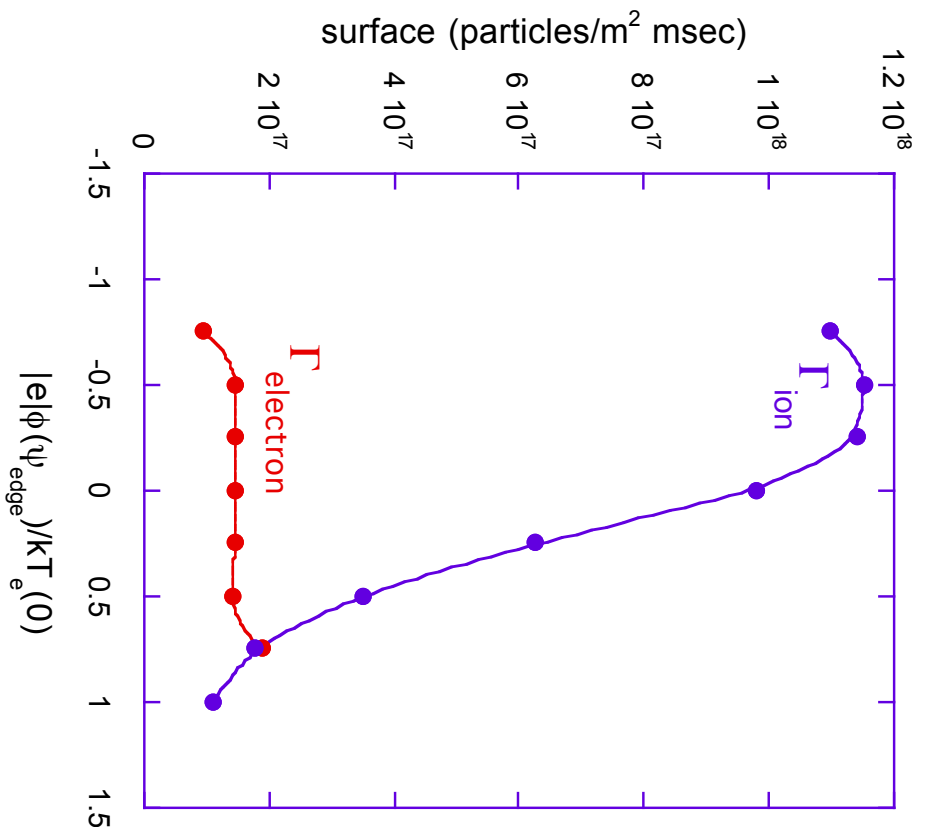
**ECH regime:**  $n(0) = 1.8 \times 10^{19} \text{ m}^{-3}$ ,  $T_e(0) = 1400 \text{ eV}$ ,  $T_i(0) = 150 \text{ eV}$   
**ICH regime:**  $n(0) = 8.3 \times 10^{19} \text{ m}^{-3}$ ,  $T_e(0) = 500 \text{ eV}$ ,  $T_i(0) = 500 \text{ eV}$



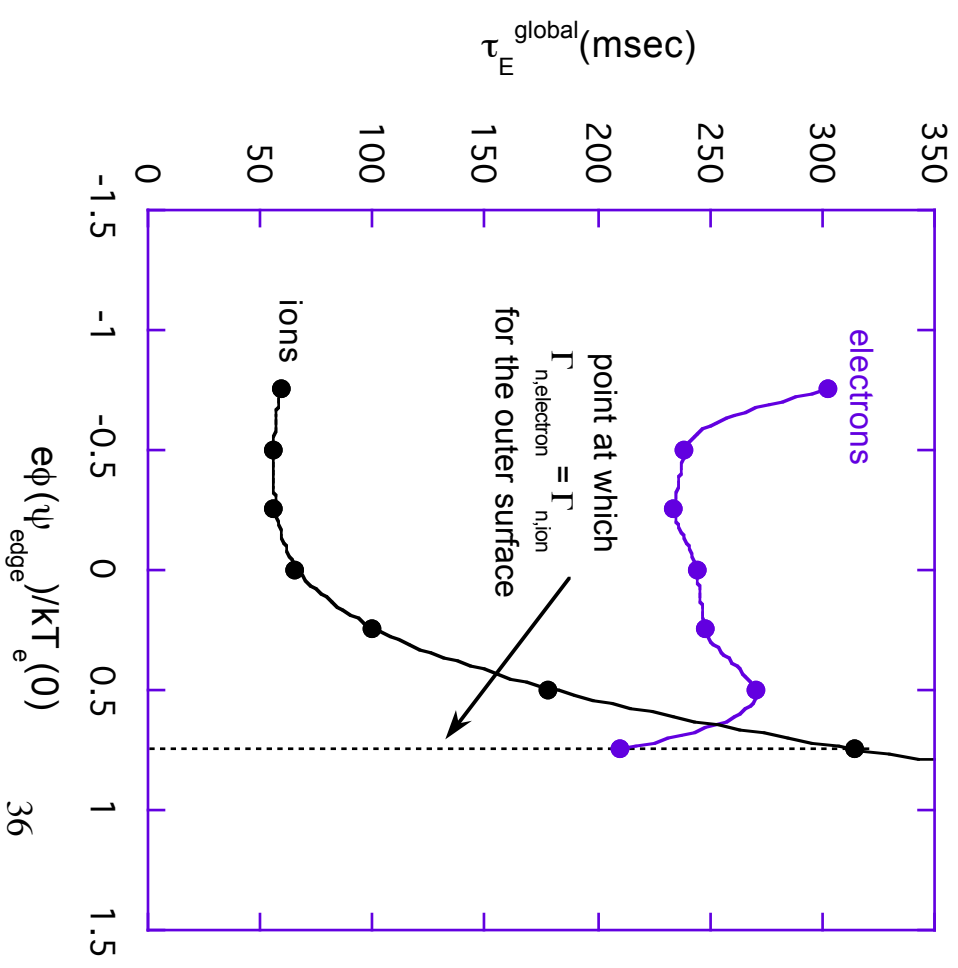
## Monte Carlo lifetimes for LCH heated gb4 configuration

$[n(0) = 8.3 \times 10^{19} \text{ m}^{-3}$ ,  $T_e(0) = 500 \text{ eV}$ ,  $T_i(0) = 500 \text{ eV}$ , flat density profile, parabolic $^{**2}$  temperature profile]

### Global ambipolarity condition [i.e., with $\square(r)$ profile fixed]

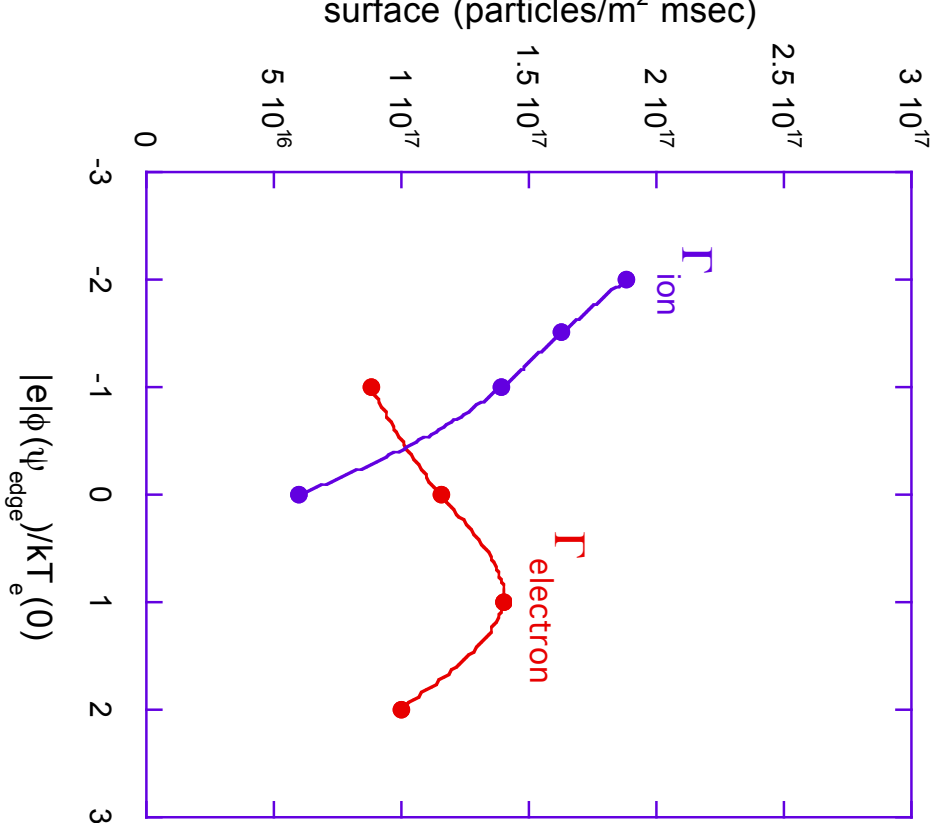


### Global electron/ion energy lifetimes

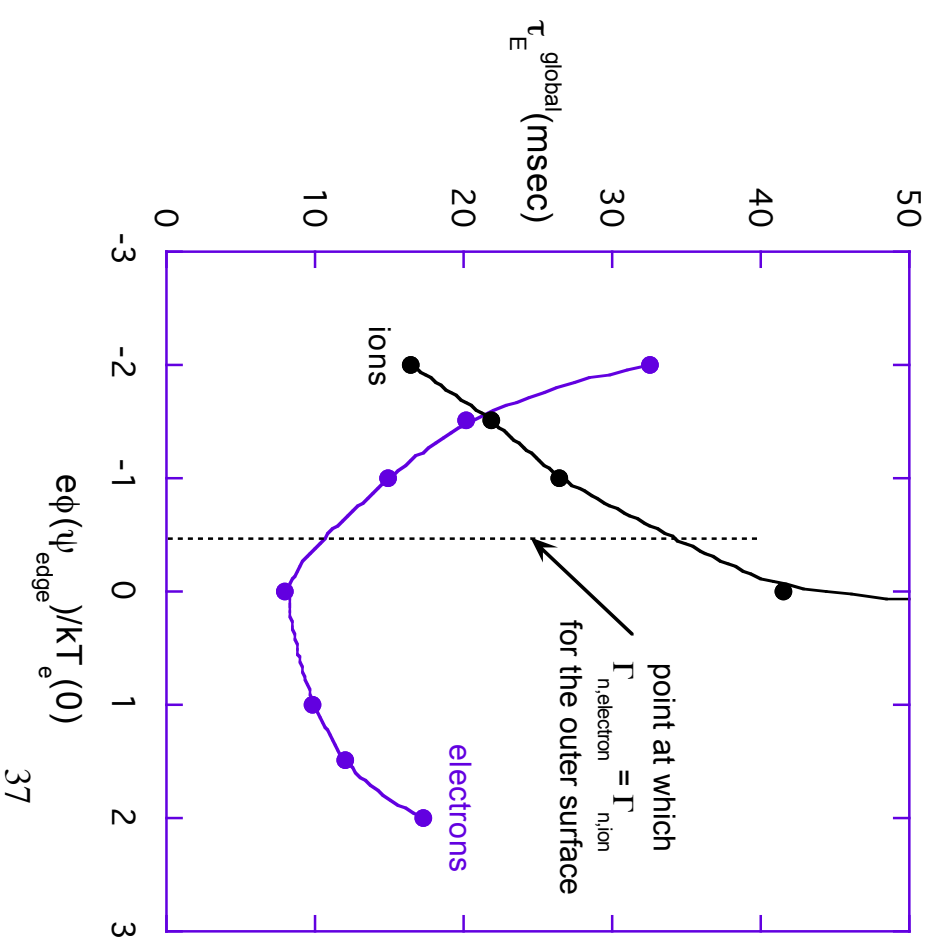


Monte Carlo lifetimes for ECH heated gb4 configuration  
 $[n(0) = 1.8 \times 10^{19} \text{ m}^{-3}, T_e(0) = 1400 \text{ eV}, T_i(0) = 150 \text{ eV, flat density profile, parabolic}^{**2} \text{ temperature profile}]$

### Global ambipolarity condition [i.e., with $\square(r)$ profile fixed]



### Global electron/ion energy lifetimes

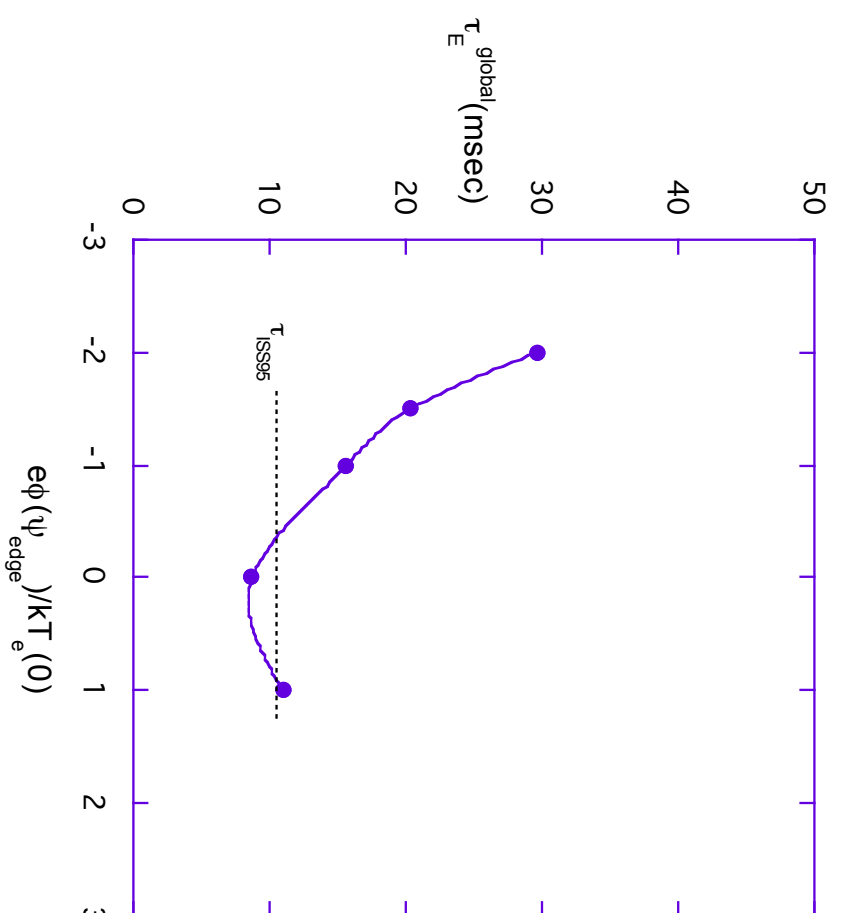


Comparison of ECH/ICH global lifetimes with ISS95 scaling law for GB4 configuration

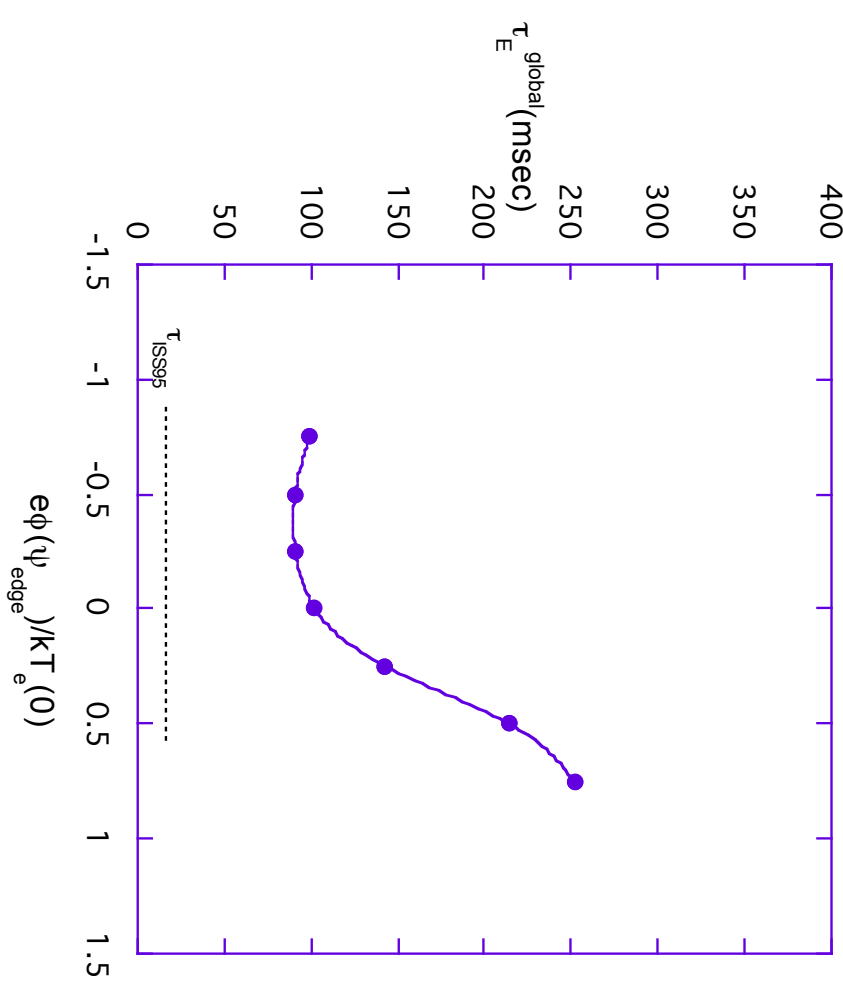
$\square_{gl}^{MC}$  = global lifetime, taking into account electron and ion loss channels:

$$\square_{gl}^{MC} = \frac{(T_e + T_i)\square_e\square_i}{T_e\square_i + T_i\square_e}$$

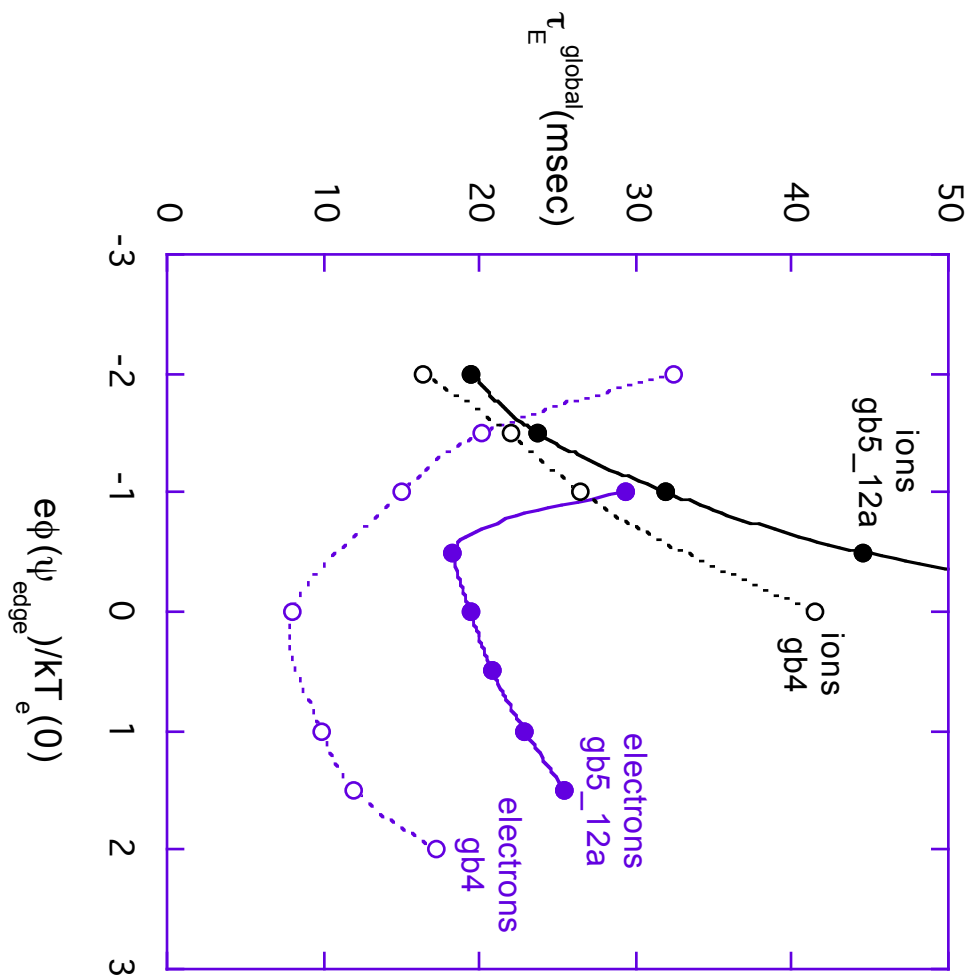
ECH heated gb4 case



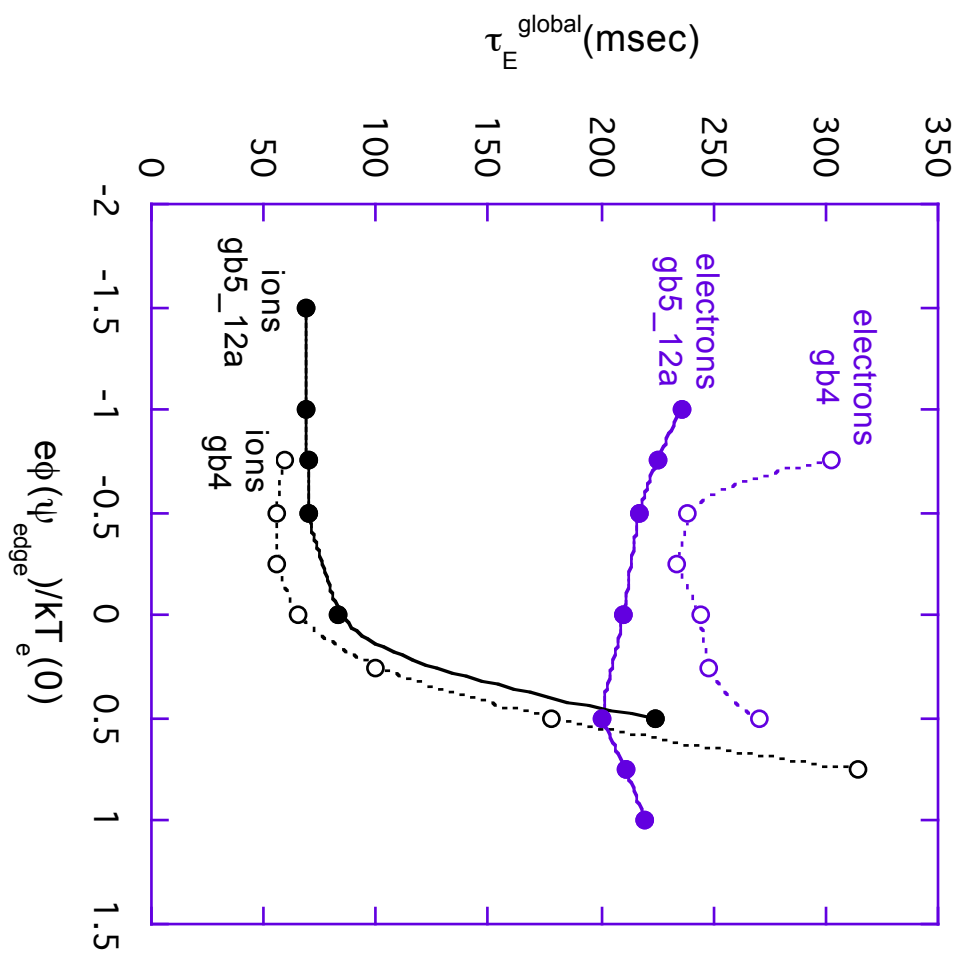
ICH heated gb4 case



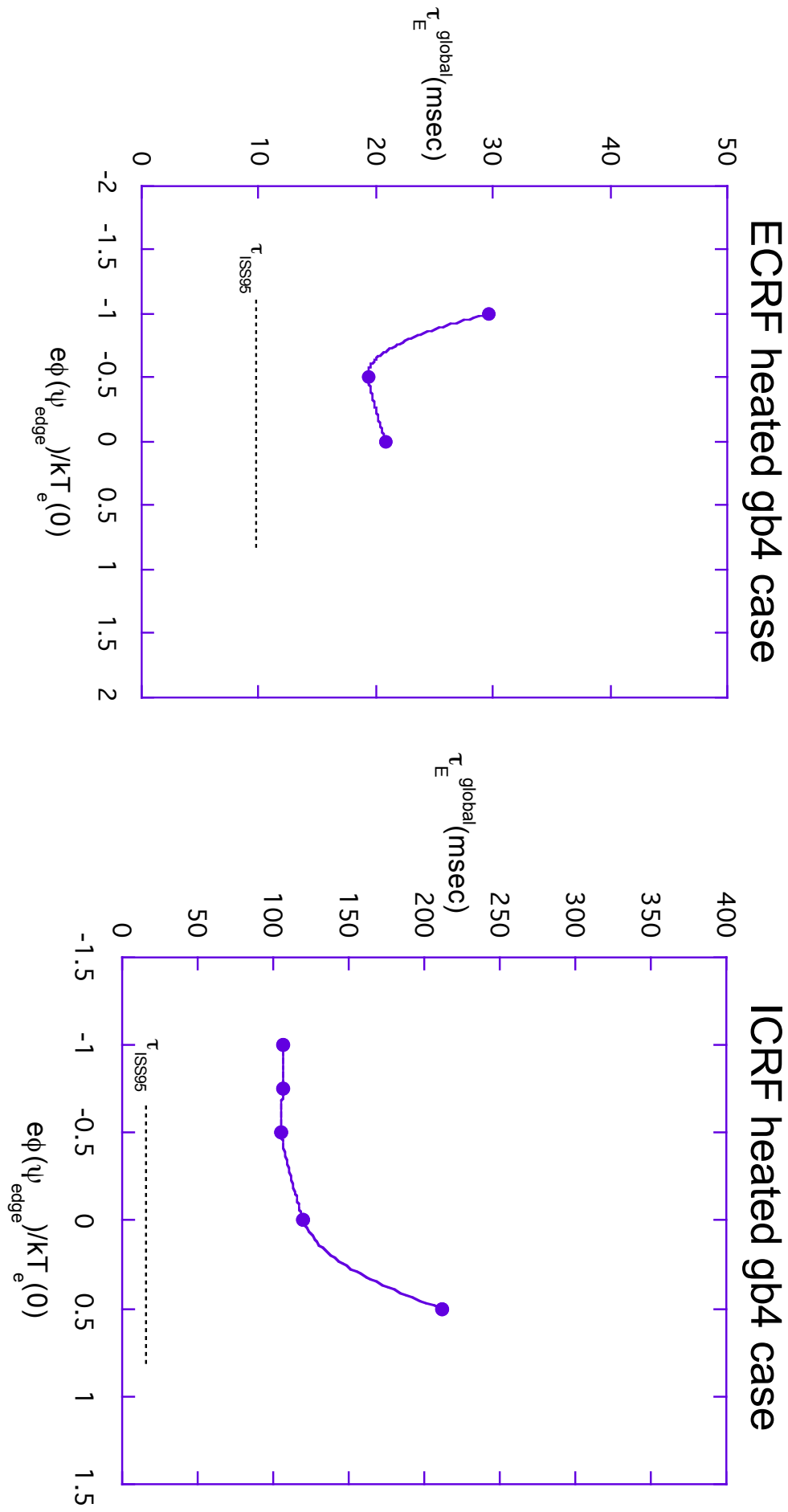
## Comparison of gb4 and gb5 global lifetimes for ECH parameters



## Comparison of gb4 and gb5 global lifetimes for ICH parameters

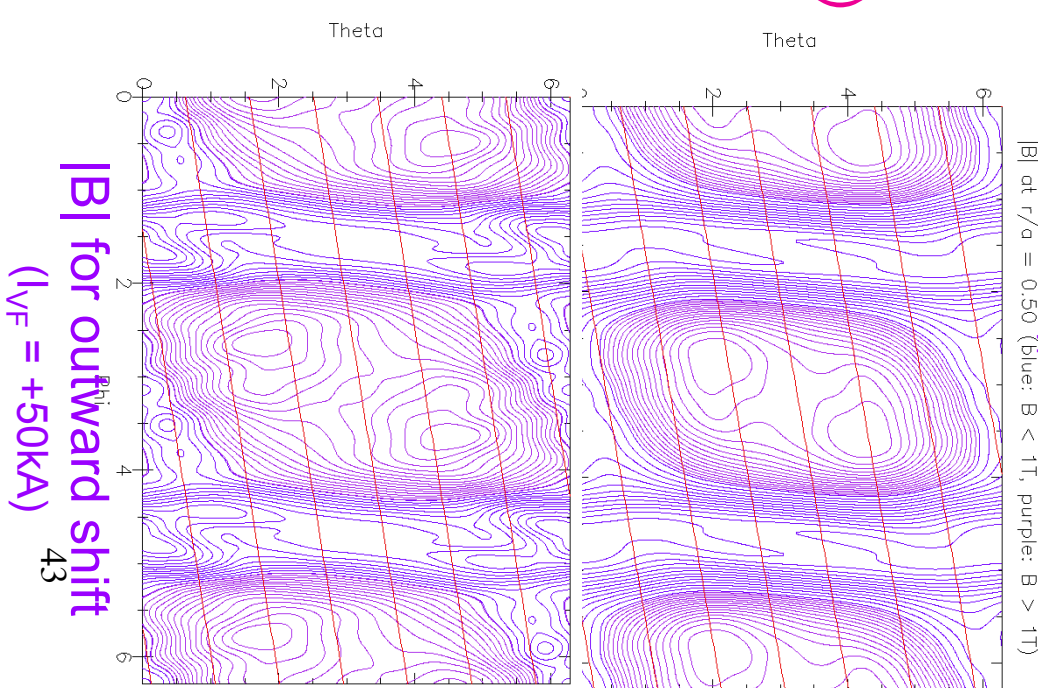
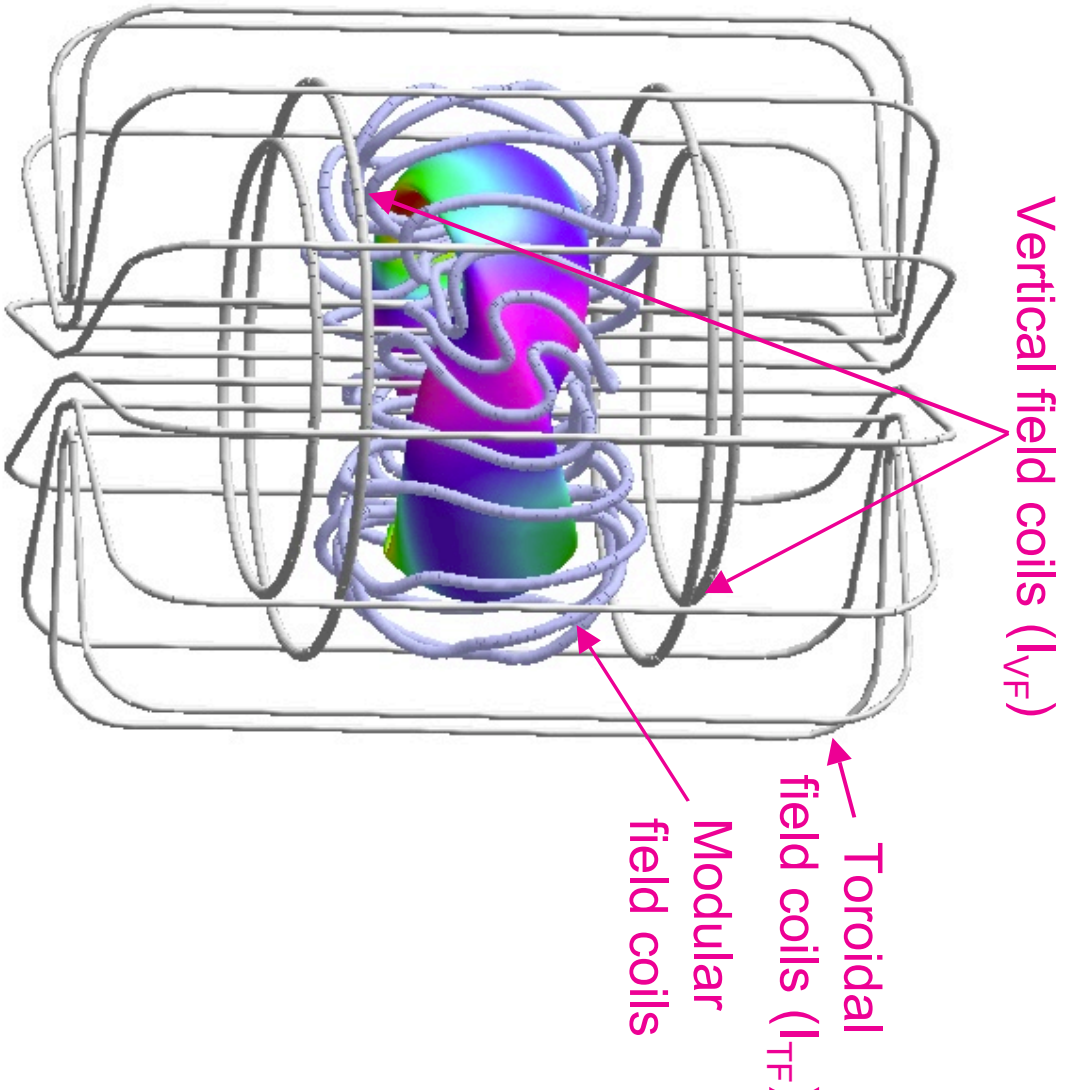


## Comparison of ECH/ICH global lifetimes with ISS95 scaling law for GB5\_12A configuration



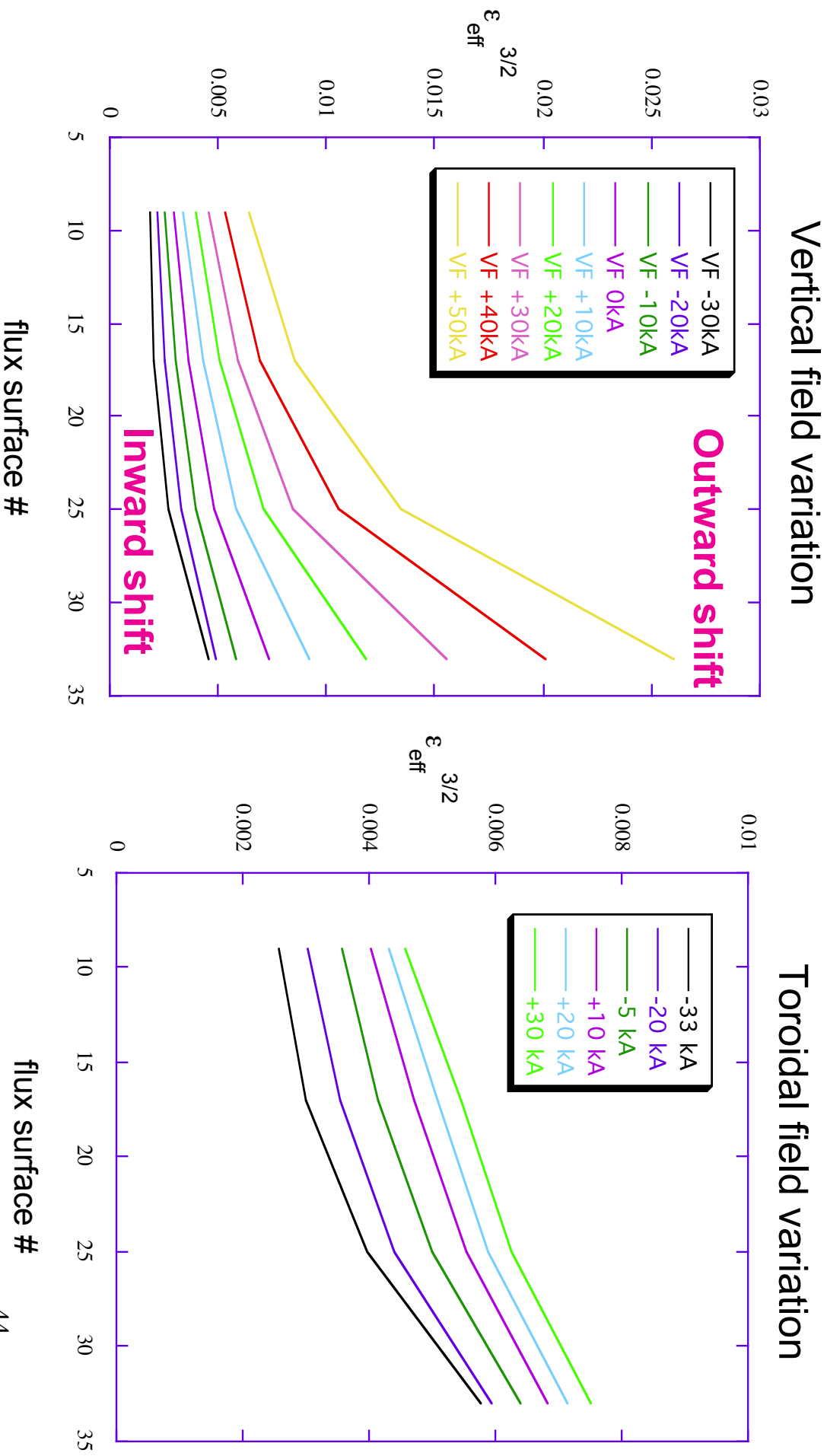
# *QPS FLEXIBILITY STUDIES*

**Flexibility is provided in QPS by 3 main coilsets.  
By changing these coil currents, different  
configurations are possible.**



**$|B|$  for outward shift  
( $I_{VF} = +50\text{kA}$ )**

**Transport properties can be influenced either by varying the vertical or toroidal fields.**



## Conclusions

- QPS should be able to reach the plasma performance needed for its mission
- ISS95 scaling + ripple transport (0-D and 1-D) predict good performance
- Monte Carlo calculations of neoclassical component show that it is not a limiting feature
- The current 1108a4 configuration offers flexibility through the vertical, toroidal and modular coil currents
- A spectrum of transport analysis tools has been developed which - form a good basis for supporting a future experiment